

**REMOVAL OF BISPHENOL A FROM AQUEOUS SOLUTION USING CU-NI  
NANOHYBRID SYNTHESIZED FROM *CASSIA SIAMEA***

**BY**

**AYOADE EMMANUEL ADEBARE**

**(20/56EF013)**

**A RESEARCH PROJECT SUBMITTED TO THE DEPARTMENT OF INDUSTRIAL  
CHEMISTRY, FACULTY OF PHYSICAL SCIENCES, UNIVERSITY OF ILORIN, KWARA  
STATE, NIGERIA.**

**IN PARTIAL FULFILMENT OF THE REQUIREMENTS FOR THE AWARD OF  
BACHELOR OF SCIENCES (B.Sc Hons) DEGREE IN INDUSTRIAL CHEMISTRY AT THE  
UNIVERSITY OF ILORIN.**

**AUGUST, 2025**

### CERTIFICATION

This is to certify that this project work was carried out by AYOADE, EMMANUEL ADEBARE (20/56EF013) and is approved as meeting the requirements for the award of Bachelor of Sciences (B.Sc. Hons) Degree in Industrial Chemistry of the Department of Industrial Chemistry, Faculty of Physical Sciences, University of Ilorin, Kwara State, Nigeria

3 Aminat

Dr. Aminat A. Mohammed

(Supervisor)

24/07/2025

Date

F.O. Nwosu

Prof. F.O. Nwosu

(Head of Department)

28/07/2025

Date

Nwagwu K.M.

External Examiner


24/07/2025

Date

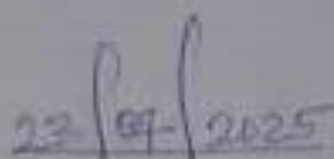
## DECLARATION

I, **AYOADE, EMMANUEL ADEBARE**, with matric number **20/56EF013**, hereby declare that this project was carried out under the supervision of Dr. Aminat A. Mohammed and its content has not been previously submitted to the department for any academic qualification.

All ideas, data, figures, and references used in this report have been properly acknowledged. The report was prepared in fulfillment of the requirements of the Department of Industrial Chemistry, University of Ilorin. I also confirm that the work was not plagiarized and has been thoroughly checked using plagiarism and AI detection tools to ensure its authenticity and integrity.



Signature



Date

## **DEDICATION**

This project work is dedicated to Almighty God for His grace bestowed upon me, His inexhaustible mercies, protection, and for the provision of all the good things life has to offer. And to my mother, Mrs. F.B. Ayoade, for her everyday moral and financial support.

## **ACKNOWLEDGEMENT**

I give all praises unto Almighty God, the giver of life and all wisdom, who has given me the privilege to be alive, grow, and reach this level successfully.

I appreciate the jewel of inestimable value, who gave birth to me and remains my pillar of strength my dynamic, ever-supporting mother. I appreciate all your efforts toward my all-around growth.

I would also like to thank all the staff members of the Department of Industrial Chemistry at the University of Ilorin for the opportunity to study and earn a Bachelor's degree in Industrial Chemistry. Amongst these very vibrant lecturers, I would like to appreciate the head of the Department, Prof F.O. Nwosu, for his fatherly and scholarly advice each time. I especially appreciate my level adviser, who doubled as my supervisor (Dr. Aminat A. Mohammed), greatly for all she has done to make sure this small boy does well in school, and of course, all other members of staff, who this list cannot contain, are highly appreciated. Thank you all for giving me the ground to study and flourish.

Finally, I would like to appreciate all my classmates and research colleagues, thank you all. God bless you all.

## **TABLE OF CONTENTS**

<b>Title page</b>	<b>i</b>
Certification	ii
Declaration	iii
Dedication	iv
Acknowledgement	v
Table of Contents	vi
List of figures	xi
List of Tables	xiii
Abstract	xiv
<b>CHAPTER ONE</b>	<b>1</b>
1.1 Background of the Study	1
1.1.1 Bisphenol A (BPA) and Its Environmental Impact	1
1.1.2 Existing Techniques for the Removal of BPA	2

1.1.3 Significance of Remediation (with Types) in the Removal of BPA	2
1.1.4 Nanohybrids	3
1.1.5 Utilization of <i>Cassia siamea</i> as a Potential Nanohybrid	3
1.2 Statement of Research Problem	4
1.3 Justification of the Study	4
1.4 Aim and Objectives of the Study	5
1.5 Scope of the Study	6
1.6 LITERATURE REVIEW OF PREVIOUS STUDIES	6
1.6.1 Overview of Bisphenol A (BPA)	6
1.6.2 Nanohybrids	8
1.6.3 Adsorption technique using nanohybrids	12
1.6.4 Adsorption Isotherms	14
1.6.5 Applications of Adsorption Isotherms in Environmental Remediation	17
1.6.6 Characterization Techniques for Nanohybrid Evaluation	18
1.6.7 Advantages of Nanohybrids Adoption Over Other Methods	19

1.6.8 Emerging Trends in Remediation	19
1.6.9 <i>Cassia siamea</i> in Scientific Applications	20
<b>CHAPTER TWO</b>	<b>21</b>
2.1 Materials	21
2.2 Reagents	21
2.3 Apparatus/Equipment	21
2.4 Methodology	22
2.4.1 Sample collection	22
2.4.2 Preparation of extracts	22
2.4.3 Preparation of 0.057M Copper-Nickel Solution	23
2.4.4 Green synthesis of Copper-Nickel nanohybrids	23
2.5 Methodology for the adsorption of Bisphenol A using Copper-Nickel nanohybrids	24
2.5.1 Preparation of stock solution	24
2.5.2 Determination of Standard Curve	24
2.5.3 Effect of Concentration	25



2.5.4 Effect of Contact Time	25
2.5.5 Effect of pH	26
2.5.6 Effect of Dosage variation	26
2.5.6 Effect of Temperature	27
2.6 Characterization techniques	28
2.6.1 Extract Characterization	28
2.6.2 Nanohybrid Characterization (Before adsorption)	28
2.6.3 After adsorption Characterization	29
<b>CHAPTER THREE</b>	<b>30</b>
3.1 Characterization of <i>Cassia siamea</i> extract	30
3.2 Adsorption Analysis Characterization	31
3.2.1 Determination of the wavelength of maximum absorbance	31
3.2.2 Determination of Calibration Curve	32
3.2.3 Effect of concentration	33
3.2.4 Effect of Contact Time	34

3.2.5 Effect of pH	34
3.2.6 Effect of Dosage Variation	35
3.2.7 Effect of Temperature	36
3.3 Characterization of the Synthesized Copper-Nickel Nanohybrids	37
3.3.1 FTIR (Fourier-Transform infrared spectroscopic):	37
3.3.2 Scanning Electron Microscopy	40
3.3.3 X-Ray diffraction	43
3.5 Adsorption Isotherms Modeling	46
3.5.1 Langmuir Isotherm	46
3.5.2 Freundlich Isotherm	47
3.5.3 Temkin Isotherm	48
3.5.4 Comparative Evaluation and Bioremediation Implications	49
4.1 Conclusion	51
4.2 Recommendation	52
<b>REFERENCES</b>	<b>55</b>

## LIST OF FIGURES

Figure 1: Structure of Bisphenol A	1
Figure 2: FTIR Spectrum of <i>Cassia siamea</i> Extract	31
Figure 3: Curve of showing the maximum absorbance of BPA as 260nm	32
Figure 4: Calibration curve of the Stock Solution	32
Figure 5: (a) Curve showing the concentration of BPA before and after adsorption (b) Adsorption capacity curve showing the optimum concentration for the adsorption of BPA as 60 ppm	33
Figure 6: (a) Curve relating time variation of the concentration of BPA before and after adsorption, (b) Adsorption capacity curve showing the optimum time for the adsorption of BPA as 4h	34
Figure 7: (a) Curve relating pH variation to concentration of BPA before and after adsorption, (b) Adsorption capacity curve showing the optimum pH for the adsorption of BPA as 6-7.	35
Figure 8: (a) Curve relating dosage variation to concentration of BPA before and after adsorption, (b) Adsorption capacity curve showing the optimum mass for adsorption of BPA as 0.04g	36
Figure 9:(a) Curve relating Temperature variation to concentration of BPA before and after adsorption, (b) Adsorption capacity curve showing the optimum temperature for the adsorption of BPA as 60 °C.	37
Figure 10: FTIR spectra of the synthesized Cu-Ni nanohybrids	38

Figure 11: Scanning electron microscopy images of the synthesized Cu-Ni nanohybrids at different magnifications.	42
Figure 12: X-ray diffraction of synthesized Cu-Ni nanohybrid.	44
Figure 13 FT-IR spectrum of the synthesized nanohybrid after adsorption	39
Figure 14: Scanning electron microscopy images of the synthesized Cu-Ni nanohybrids at different magnifications (100nm, 200nm) after adsorption.	43
Figure 15: X-ray diffraction of Cu-Ni nanohybrids after adsorption	45

## LIST OF TABLES

Table 1: Major bands observed for the Cassia siamea extract	31
Table 2: Major bands observed for the synthesized Cu-Ni nanohybrids	38
Table 3: Table comparing the peak of Cu-Ni nanohybrid before and after adsorption	40
Table 4: Summary of Isotherm Model Parameters and Fit Quality	50

## ABSTRACT

Bisphenol A (BPA), a widely used industrial chemical, poses significant environmental and health risks due to its persistence and endocrine-disrupting properties. This study presents a green synthesis approach for copper-nickel (Cu-Ni) nanohybrids using *Cassia siamea* leaf extract, aimed at efficient BPA removal from aqueous solutions. The phytochemicals in *Cassia siamea* served as natural reducing and stabilizing agents, enabling eco-friendly nanohybrids without toxic reagents.

Characterization of the nanohybrids via FTIR, SEM, XRD, and UV-Vis spectroscopy confirmed their structural integrity and suitability for adsorption applications. Batch adsorption experiments were conducted to assess the influence of BPA concentration, contact time, pH, adsorbent dosage, and temperature. Optimal removal was achieved at 60 ppm BPA concentration, pH 6–7, 4 hours contact time, 0.04 g dosage, and 60°C temperature.

Adsorption isotherm modeling revealed that the Langmuir model best described the process, indicating monolayer adsorption on a homogeneous surface. Freundlich and Temkin models also provided insights into multilayer interactions and adsorption energetics. Post-adsorption analysis confirmed strong binding between BPA molecules and the nanohybrid surface.

The results demonstrate that *Cassia siamea*-derived Cu-Ni nanohybrids are a promising, sustainable, and cost-effective material for BPA remediation. This work contributes to the

development of green nanotechnology for environmental purification and offers scalable solutions for water treatment in resource-limited regions.

**Keywords:** Bisphenol A, *Cassia siamea*, nanohybrids, adsorption.

## CHAPTER ONE

### INTRODUCTION

#### 1.1 Background of the Study

##### 1.1.1 Bisphenol A (BPA) and Its Environmental Impact

Bisphenol A (BPA) is an industrial chemical extensively used in the production of polycarbonate plastics and epoxy resins. These materials are commonly found in water bottles, food containers, medical devices, and coatings for metal cans. Due to its widespread use, BPA is frequently released into the environment, primarily through industrial effluents, plastic degradation, and landfill leachates. BPA is classified as an endocrine disruptor, interfering with hormonal systems in humans and wildlife, leading to adverse health effects such as reproductive disorders, metabolic diseases, and carcinogenic risks. Additionally, BPA contamination in water bodies poses a severe threat to aquatic ecosystems, leading to bioaccumulation in aquatic organisms and further entering the food chain.

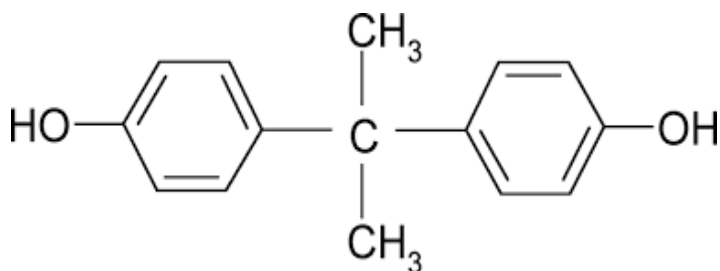


Figure 1: Structure of Bisphenol A (*Cheng & Wang, 2024*)



### 1.1.2 Existing Techniques for the Removal of BPA

Various conventional techniques are employed for BPA removal from contaminated environments, including:

- i. **Chemical Oxidation:** This method utilizes oxidizing agents such as ozone and chlorine to break down BPA. However, it often yields toxic by-products and requires a high energy input.
- ii. **Adsorption:** Activated carbon and biochar are commonly used to adsorb BPA from water. While effective, their regeneration and disposal pose environmental challenges.
- iii. **Advanced Oxidation Processes (AOPs):** These involve hydroxyl radicals to degrade BPA, including Fenton oxidation and photocatalysis. However, they demand high operational costs and continuous monitoring.
- iv. **Biological Methods:** Microbial degradation of BPA through bacteria and fungi presents an eco-friendly alternative but requires optimization for efficiency.

### 1.1.3 Significance of Remediation (with Types) in the Removal of BPA

Remediation offers a cost-effective and environmentally friendly approach to BPA removal by utilizing biological organisms, such as bacteria, fungi, or plants, to degrade contaminants. The main types of bio remediation include in situ remediation, where treatment occurs at the contaminated site without excavation. Examples include bioventing and bioaugmentation, ex situ remediation (contaminated material is removed and treated in a controlled environment, such as

bioreactors or land farming). Other types include Bioaugmentation, Bio-stimulation, and Phytoremediation. These Remediation strategies are considered promising for BPA removal, particularly when coupled with advanced materials such as nanohybrids.

#### **1.1.4 Nanohybrids**

Nanohybrids are composite materials that incorporate nanohybrids with organic or inorganic matrices to enhance their physicochemical properties. These materials exhibit high surface area, reactivity, and stability, making them suitable for various applications, including environmental remediation. The use of nanohybrids in Remediation can improve microbial efficiency, catalyze degradation reactions, and enhance pollutant removal from aqueous environments.

Nanohybrids play a crucial role in remediation by acting as catalysts to accelerate pollutant breakdown, enhancing microbial adhesion and enzymatic activity, improving adsorption efficiency for pollutants, and providing a stable medium for sustained remediation. Nanohybrids enhance BPA degradation efficiency by offering a larger surface area for microbial interaction and reducing BPA toxicity through catalytic processes.

#### **1.1.5 Utilization of *Cassia siamea* as a Potential Nanohybrid**

*Cassia siamea* (Cassia) has been identified as a potential source for nanohybrid synthesis due to its rich bioactive compounds, including polyphenols and flavonoids. These compounds exhibit strong reducing and stabilizing properties, making them ideal for green nanomaterial synthesis. Cassia-based nanohybrids offer the advantages of sustainability, cost-effectiveness, and enhanced Remediation efficiency. The natural antioxidants and metal-binding properties of

Cassia facilitate the synthesis of eco-friendly Cu-Ni nanohybrids capable of degrading BPA in contaminated water bodies. (Ali *et al.*,2020)

## **1.2 Statement of Research Problem**

BPA contamination in water sources remains a significant environmental and public health concern. Existing remediation techniques often fall short due to high costs, incomplete degradation, and potential secondary pollution. Developing an eco-friendly, efficient, and sustainable method for BPA removal is imperative. The utilization of *Cassia siamea*-based Cu-Ni nanohybrids provides a novel and promising approach to address these challenges.

## **1.3 Justification of the Study**

The rationale for this study lies in its environmental significance, scientific novelty, and socio-economic viability. Bisphenol A (BPA) has emerged as a global pollutant due to its persistence in aquatic ecosystems and its endocrine-disrupting effects on both humans and wildlife. Existing remediation techniques, while effective, often rely on harsh chemicals, energy-intensive operations, and high financial costs, underscoring the need for more sustainable alternatives.

This research proposes the use of copper-nickel (Cu-Ni) nanohybrids synthesized via *Cassia siamea* leaf extract as a green and cost-effective solution for BPA remediation. The environmental relevance of this approach is evident in its potential to mitigate BPA contamination, which threatens biodiversity and public health. By employing a plant-based synthesis method, the study eliminates the use of toxic solvents and

synthetic reducing agents, thereby promoting sustainability and reducing hazardous waste.

Furthermore, the use of locally available botanical resources significantly lowers production costs, making the technology accessible and scalable, particularly in resource-limited settings. Scientifically, the integration of nanotechnology with biogenic synthesis enhances the functional properties of the nanohybrids, including surface area, reactivity, and adsorption capacity. These attributes enable efficient BPA degradation through mechanisms such as adsorption, photocatalysis, and redox reactions.

In summary, this research aligns with global efforts to develop environmentally responsible and economically feasible technologies for pollution management, offering a promising pathway toward sustainable water treatment solutions.

#### **1.4 Aim and Objectives of the Study**

This study aims to synthesize and evaluate the efficiency of *Cassia siamea*-based Cu-Ni nanohybrids for the Remediation of BPA from aqueous solutions. The specific objectives include:

- i. To synthesize and characterize Cu-Ni nanohybrids using *Cassia siamea* extracts.
- ii. To assess the Remediation efficiency of the synthesized nanohybrids for BPA degradation.

- iii. To analyze the effect of variables such as pH, concentration, and time on BPA removal.
- iv. To investigate the batch adsorption process and characterize the adsorption process using different analytical techniques.
- v. To evaluate the adsorption isotherm models.

## **1.5 Scope of the Study**

This research focuses on the synthesis of Cu-Ni nanohybrids using *Cassia siamea* extracts and their application in BPA removal from aqueous environments. The study includes the laboratory-based synthesis and characterization of nanohybrids, experimental evaluation of BPA degradation efficiency, analysis of physicochemical parameters influencing the Remediation method adopted. The study aims to contribute valuable insights into the potential of nanotechnology and plant-based materials in environmental remediation, particularly in addressing BPA pollution.

## **1.6 LITERATURE REVIEW OF PREVIOUS STUDIES**

Various literature was consulted to provide a comprehensive review of BPA contamination, removal techniques, and the role of nanohybrids and *Cassia siamea* in Remediation.

### **1.6.1 Overview of Bisphenol A (BPA)**

Bisphenol A (BPA) is an industrial chemical primarily used in manufacturing polycarbonate plastics and epoxy resins, which are widely found in consumer goods such as food packaging, baby bottles, medical devices, and thermal paper receipts (Flint *et al.*, 2012). BPA, known for

its endocrine-disrupting ability, leads to potential health and environmental concerns and due to its extensive use, it has been detected in various environmental matrices, including water, soil, and biological tissues (Rochester, 2013).

BPA contamination arises from multiple anthropogenic sources, including industrial effluents, municipal wastewater, landfill leachates, and the degradation of plastic products (Staples *et al.*, 2018). Studies indicate that wastewater treatment plants are among the primary sources of BPA release into aquatic environments, as conventional treatment methods fail to completely remove BPA from wastewater (Kang *et al.*, 2006). Other sources include household plastic waste, paper coatings, and dental sealants, contributing to its widespread presence in the environment.

BPA contamination in water bodies has been widely reported worldwide, with concentrations varying depending on proximity to industrial zones and wastewater discharge points (Xue *et al.*, 2021). Research has shown BPA levels in surface and groundwater, drinking water sources, and marine ecosystems, raising concerns over its bioaccumulation and potential effects on aquatic organisms (Crain *et al.*, 2007). The persistence of BPA in water depends on factors such as pH, temperature, and microbial activity, further complicating its removal from aquatic environments (Yang *et al.*, 2017).

### **Traditional Methods for BPA Removal**

- i. **Chemical Oxidation Method:** Chemical oxidation techniques employ oxidants such as ozone, chlorine, and hydrogen peroxide to degrade BPA into less harmful by-products (Yang *et al.*, 2017). While these methods are effective in breaking down BPA, they often generate secondary

pollutants, necessitating additional treatment measures to ensure environmental safety (Tian *et al.*, 2020).

- ii. **Adsorption Technique:** Adsorption using activated carbon and biochar is widely used for BPA removal due to its high efficiency and cost-effectiveness (Li *et al.*, 2019). Recent studies have explored alternative adsorbents, such as agricultural waste-based biochar and metal-organic frameworks, to enhance BPA adsorption and improve regeneration capabilities (Zhang *et al.*, 2021).
- iii. **Advanced Oxidation Processes:** Advanced oxidation processes (AOPs) involve the generation of highly reactive hydroxyl radicals to degrade BPA (Tian *et al.*, 2020). Techniques such as Fenton oxidation, photocatalysis, and electrochemical oxidation have demonstrated high efficiency in BPA removal, but challenges such as high energy demand and operational costs remain (Ahmed *et al.*, 2017).
- iv. **Biological Remedy Technique:** Biological methods use microorganisms such as bacteria and fungi to degrade BPA through enzymatic processes (Huang *et al.*, 2019). Microbial strains, including *Sphingomonas* and *Pseudomonas*, have shown promising results in BPA biodegradation, though environmental factors such as pH and temperature influence their efficiency (Chen *et al.*, 2018).

### 1.6.2 Nanohybrids

The rapid development of nanotechnology has opened new avenues for the design of multifunctional materials tailored for applications in catalysis, energy conversion, environmental remediation, and biomedical engineering. Among these, copper-nickel (Cu-Ni)

nanohybrids represent a promising class of bimetallic structures owing to their synergistic properties, tunable morphologies, and diverse functionality. By combining the electrical conductivity and antibacterial traits of copper with the chemical stability and magnetic characteristics of nickel, Cu-Ni nanohybrids exhibit enhanced performance compared to their individual components (Aman *et al.*, 2025).

Several interrelated properties define the physicochemical behavior of Cu-Ni nanohybrids, one of the most prominent being electrical conductivity, where copper's excellent charge mobility complements nickel's resistance to corrosion, resulting in stable conductive pathways suitable for sensors and electronic devices (Bai, 2019). Furthermore, magnetic properties arise from nickel's intrinsic ferromagnetism, enabling magnetic separation and bio-imaging applications (Ghaderi *et al.*, 2022).

The catalytic activity of Cu-Ni hybrids is considerably higher than that of either metal alone, due to ensemble effects at their interface, which enhance reaction kinetics and lower activation energies. This bimetallic synergy has proven valuable in hydrogen evolution reactions, CO oxidation, and organic pollutant degradation (Skakri *et al.*, 2025). Additionally, Cu-Ni nanohybrids show pronounced antibacterial behavior and exhibit optical properties such as localized surface plasmon resonance (LSPR), which can be leveraged in biosensing and photonic applications (Aman *et al.*, 2025).



## Mode of Synthesis

Cu-Ni nanohybrids can be synthesized through a variety of methods, each influencing the resultant morphology and functionality.

- i. **Chemical Reduction** is a well-established route where reducing agents like sodium borohydride or hydrazine convert metal ions into nanohybrids. Bai (2019) employed a successive reduction technique to obtain Cu-core/Ni-shell structures, optimizing electron transfer and reactivity.
- ii. **Green Synthesis**, which utilizes plant extracts as reducing and stabilizing agents, offers a sustainable alternative. Ali *et al.* (2020) demonstrated the use of *Cassia siamea* leaf extract to fabricate Cu-Ni nanohybrids, harnessing the antioxidant-rich phytochemicals for metal ion reduction and nanohybrids stabilization.
- iii. **Electrodeposition** involves electrochemically co-depositing copper and nickel onto conductive substrates. This technique enables precise control of elemental ratios and film thickness, enhancing performance in energy-related applications (Skakri *et al.*, 2025).
- iv. **Thermal Reduction** uses high-temperature solvents to control nucleation and growth. Liu *et al.* (2017) utilized oleylamine and trioctylphosphine in a one-pot method to create uniform Cu-Ni nanospheres, demonstrating scalability and customizability.

### 1.6.2.3 Factors Influencing Synthesis

The quality and performance of Cu-Ni nanohybrids depend heavily on synthesis conditions:

- i. **Metal precursor ratios** define alloy phases, surface charge, and catalytic selectivity. Adjusting the Cu:Ni molar ratio alters electron distribution and structural stability (Liu *et al.*, 2017).
- ii. **Reaction temperature and pH** affect the rate of reduction and particle aggregation. Mild alkaline conditions promote controlled growth and reduce oxidation risks (Bai, 2019).
- iii. **Laser parameters** in PLAL—like pulse energy and wavelength—modulate particle size and morphology (Aman *et al.*, 2025).
- iv. **Phytochemical composition** in green synthesis determines reduction power and biocompatibility. Polyphenols and flavonoids are especially effective in chelating and reducing metal ions (Ali *et al.*, 2020).

These parameters must be carefully optimized to achieve uniform, high-performance nanohybrids suitable for targeted applications.

### 1.6.2.4 Applications of Cu-Ni Nanohybrids

Cu-Ni nanohybrids have demonstrated versatility across several domains, for example, in environmental remediation, they are highly effective for removing persistent organic pollutants like Bisphenol A (BPA). Their reactive surfaces and biogenic coatings facilitate adsorption and catalytic degradation, as seen in plant-mediated synthesis approaches (Ali *et al.*, 2020).

In catalysis, Cu-Ni hybrids are instrumental in hydrogen evolution reactions (HER), methane steam reforming, and CO oxidation due to their high surface-to-volume ratio and enhanced electron transfer properties (Skakri *et al.*, 2025; Kovalskii *et al.*, 2020).

In sensor technology, Ghaderi *et al.* (2022) reported Cu-Ni bilayer nanohybrids functioning as efficient CO gas sensors at room temperature, exploiting their LSPR features and conductive responsiveness.

Biomedical applications include antibacterial coatings, drug delivery, and magnetic hyperthermia. The bimetallic composition enhances antimicrobial efficacy while allowing for remote magnetic manipulation (Aman *et al.*, 2025).

In electronics and printed films, Cu-Ni nanohybrids offer durable, conductive surfaces that resist oxidation, providing long-term stability for flexible circuits and nanodevices (Bai, 2019).

### **1.6.3 Adsorption technique using nanohybrids**

Adsorption has emerged as a widely accepted method due to its simplicity, cost-effectiveness, and high removal efficiency for a broad spectrum of contaminants. In recent years, nanohybrid engineered materials composed of two or more nanoscale components have gained significant attention as advanced adsorbents for environmental remediation.

Adsorption is a surface phenomenon where pollutants adhere to the surface of a solid material. The efficiency of this process depends on the adsorbent's surface area, pore structure, and the nature of its functional groups. Nanohybrids enhance these properties by combining the strengths

of individual nanomaterials, such as metal oxides, carbon-based structures, and biopolymers, resulting in synergistic effects that improve adsorption capacity and selectivity (Ibrahim *et al.*, 2022).

For instance, metal-organic frameworks (MOFs) anchored on cellulose nanofibers have demonstrated high adsorption capacities for heavy metals due to their porous architecture and functional diversity (Singh *et al.*, 2025). Similarly, biochar modified with nanomaterials such as ZnS or MnO<sub>2</sub> exhibits enhanced surface functionality and active sites, leading to improved adsorption of heavy metals like lead and cadmium (Ahuja *et al.*, 2022).

Nanohybrids facilitate pollutant removal through multiple mechanisms, including electrostatic attraction, hydrogen bonding,  $\pi$ - $\pi$  interactions, and surface complexation. These interactions are influenced by the physicochemical properties of the nanohybrid, such as surface charge, functional group density, and pore size distribution (Katiyar & Katiyar, 2023). For example, carbon nanotube-based nanohybrids have shown exceptional adsorption rates for Cu(II) and Cr(VI), reaching capacities of up to 341 mg/g due to their high surface area and layered structure (Ibrahim *et al.*, 2022).

Nanohybrids have been successfully applied in the removal of various pollutants, including heavy metals, dyes, pharmaceuticals, and endocrine-disrupting compounds like Bisphenol A (BPA). Their performance is often evaluated using adsorption isotherms (e.g., Langmuir and Freundlich models) and kinetic studies (e.g., pseudo-first-order and pseudo-second-order models). Optimization techniques such as Response Surface Methodology (RSM) have been

employed to fine-tune synthesis parameters and maximize adsorption efficiency (Singh *et al.*, 2025).

In one study, MOF-cellulose nanohybrids synthesized from rice straw achieved a maximum Cu(II) adsorption capacity of 263.5 mg/g, with a removal efficiency of 82.8% and recyclability over ten cycles with minimal loss in performance (Singh *et al.*, 2025). Such results underscore the potential of nanohybrids in scalable and sustainable water treatment solutions.

#### **1.6.4 Adsorption Isotherms**

Adsorption isotherms are mathematical models that describe the interaction of solutes with adsorbent surfaces at equilibrium under constant temperature. These models are crucial for understanding the adsorption mechanism, optimizing the performance of adsorbents, and designing efficient treatment systems for environmental remediation. In the context of nanohybrids and pollutant removal, adsorption isotherms provide critical insights into surface affinity, capacity, and interaction dynamics between adsorbate and adsorbent.

An adsorption isotherm expresses the relationship between the amount of adsorbate adsorbed per unit mass of adsorbent ( $Q_e$ ) and its equilibrium concentration in solution ( $C_e$ ). This relationship helps determine whether adsorption occurs via monolayer coverage, multilayer accumulation, or heterogeneous surface interactions. Isotherms also reveal whether the process is governed by physical forces (physisorption) or chemical bonding (chemisorption) (Ahmed *et al.*, 2023).

Some Common Isotherm Models are:

#### 1.6.4.1 Langmuir Isotherm

The Langmuir model assumes monolayer adsorption on a homogeneous surface with finite identical sites. It is expressed as:

$$Q_e = \frac{Q_m K_i C_e}{1 + K_i C_e} \quad (1)$$

$$\frac{C_e}{Q_e} = \frac{C_e}{Q_m} + \frac{1}{K_i Q_m} \quad (2)$$

Where:  $Q_e$  = amount adsorbed at equilibrium (mg/g)

$$Q_e = \frac{(C_b - C_a)V}{M} \quad (3)$$

$C_e$  = equilibrium concentration

$Q_m$  = maximum adsorption capacity (mg/g)

$K_i$  = Langmuir constant related to adsorption energy

$C_o$  = Concentration before adsorption (as in  $C_o$ )

$C_a$  = Concentration after adsorption (as in  $C_e$ )

$V$  = Volume of adsorbate used

$M$  = Mass of adsorbent

This model is widely used for systems where adsorbate molecules do not interact with each other and adsorption occurs uniformly (Murphy *et al.*, 2023).

#### 1.6.4.2 Freundlich Isotherm

The Freundlich model describes adsorption on heterogeneous surfaces and allows for multilayer adsorption. It is given by:

$$q_e = K_f C_e^{1/n} \quad (4)$$

$$\log Q_e = \log K_f + (1/n) \log C_e \quad (5)$$

Where:

$K_f$  is the Freundlich constant indicating adsorption capacity

$1/n$  is the heterogeneity factor; values between 0 and 1 indicate favorable adsorption

This empirical model is suitable for complex systems with varying surface energies (Sari *et al.*, 2009).

#### 1.6.4.3 Temkin Isotherm

Temkin accounts for adsorbent–adsorbate interactions and assumes that the heat of adsorption decreases linearly with coverage. It is expressed as:

$$q_e = B \ln(A_T C_e) \quad (6)$$

$$Q_e = B \ln A_T + B \ln C_e \quad (7)$$

Where:  $B$  = constant related to adsorption heat

$A_T$  = Temkin isotherm constant

This model is useful for systems where adsorbate - adsorbent interactions influence adsorption energetics (Khan, 2000)

### **Model Selection and Data Fitting**

Choosing the appropriate isotherm model depends on the nature of the adsorbent, the adsorbate, and experimental conditions. Researchers often use linear and nonlinear regression to fit experimental data to isotherm equations. Nonlinear methods are preferred for accuracy, as linearization can lead to distorted parameter estimation (Ayawei *et al.*, 2017).

Error functions such as sum of squared errors (SSE), chi-square ( $\chi^2$ ), and average relative error (ARE) are used to evaluate model fit. The model with the lowest error and highest correlation coefficient ( $R^2$ ) is considered best suited for describing the system (Ahmed *et al.*, 2023).

#### **1.6.5 Applications of Adsorption Isotherms in Environmental Remediation**

Adsorption isotherms are crucial in designing systems for removing pollutants like heavy metals, dyes, and endocrine disruptors such as Bisphenol A (BPA). For instance, Cu-Ni nanohybrids synthesized using *Cassia siamea* have shown high affinity for BPA, with adsorption behavior fitting the Langmuir model, indicating monolayer coverage and uniform surface interaction (Ali *et al.*, 2020).

Isotherm modeling also aids in estimating adsorbent dosage, predicting breakthrough curves in column studies, optimizing contact time, and surface area, and comparing adsorbent performance across materials



#### 1.6.6 Characterization Techniques for Nanohybrid Evaluation

Accurate characterization is essential for validating the synthesis and functionality of nanomaterials used in environmental remediation. In this study, Cu-Ni nanohybrids synthesized using *Cassia siamea* were analyzed using four complementary techniques: Fourier Transform Infrared Spectroscopy (FTIR), Scanning Electron Microscopy (SEM), Energy Dispersive X-ray Spectroscopy (EDX), and X-ray Diffraction (XRD).

- i. **FTIR** was employed to identify functional groups and confirm the presence of phytochemicals from *Cassia siamea* involved in nanohybrids stabilization. Characteristic peaks corresponding to hydroxyl, carbonyl, and aromatic groups indicated successful capping and reduction of metal ions, validating the green synthesis approach (Eid, 2022; Escobar Barrios *et al.*, 2012).
- ii. **SEM** provided high-resolution images of the nanohybrids, revealing surface morphology, particle shape, and agglomeration tendencies. The micrographs showed uniformly distributed particles with porous structures, favorable for adsorption applications (Akhtar *et al.*, 2018; Santos *et al.*, 2022).
- iii. **EDX**, integrated with SEM, enabled elemental analysis of the nanohybrids. It confirmed the incorporation of copper and nickel into the hybrid matrix and detected trace elements that may influence catalytic behavior (Mahapatro, 2022; Santos *et al.*, 2022).
- v. **XRD** was employed to determine the crystalline structure and phase composition of the synthesized materials. Distinct diffraction peaks matched standard patterns for Cu-Ni alloys, and the calculated crystallite size using the Scherrer equation indicated nanoscale

dimensions. The presence of sharp peaks confirmed high crystallinity, essential for photocatalytic and adsorptive efficiency (Ortiz Ortega *et al.*, 2022; Santos, 2022).

Together, these techniques provided a comprehensive understanding of the nanohybrids' physicochemical properties, supporting their suitability for Bisphenol A removal from aqueous environments

#### **1.6.7 Advantages of Nanohybrids Adoption Over Other Methods**

Nanohybrids offer advantages such as high stability, reusability, and superior adsorption capacity compared to conventional materials (Das *et al.*, 2021). Their application in Remediation enhances pollutant degradation efficiency, making them a promising alternative for BPA removal.

#### **1.6.8 Emerging Trends in Remediation**

Microbial biodegradation of BPA is facilitated by specific enzymes such as laccases, peroxidases, and monooxygenases, which catalyze BPA breakdown into non-toxic metabolites (Chen *et al.*, 2018). Genetic engineering approaches are being explored to enhance microbial degradation efficiency, particularly in complex environmental conditions (Abraham *et al.*, 2021).

Another recent trend is the use of bio-based materials, such as lignocellulosic biomass, algal extracts, and polysaccharide-based materials, which have gained attention for their potential in Remediation (Abraham *et al.*, 2021). These materials offer biodegradable, sustainable, and

cost-effective alternatives for BPA removal, often enhancing microbial activity and adsorption capabilities.

#### **1.6.9      *Cassia siamea* in Scientific Applications**

*Cassia siamea* is a widely available and sustainable plant known for its medicinal and industrial applications. Its bioactive compounds contribute to its role in green nanomaterial synthesis, offering an eco-friendly approach for environmental remediation (Siddhuraju, 2007).

The presence of polyphenols, flavonoids, and tannins in *Cassia siamea* enhances its antioxidant and metal-reducing properties, making it an excellent candidate for nanohybrid synthesis (Siddhuraju, 2007). These bioactive compounds facilitate the reduction and stabilization of nanohybrids, improving their efficiency in pollutant removal.

## CHAPTER TWO

### MATERIALS AND METHODOLOGY

#### 2.1 Materials

- i. *Cassia siamea* leaves
- ii. Bisphenol A

#### 2.2 Reagents

- i. Distilled water
- ii. Copper and nickel salts
- iii. 0.1M Hydrochloric acid (HCl)
- iv. 0.1M Sodium Hydroxide (NaOH)
- v. Absolute ethanol

#### 2.3 Apparatus/Equipment

- i. 250/500mL conical flasks
- ii. 1000mL standard flask
- iii. Stirring rod
- iv. Spatula
- v. 100mL measuring cylinder
- vi. Funnel
- vii. Aluminum foil paper
- viii. Mortar and pestle
- ix. Weighing balance
- x. Paper tape
- xi. Sample bottles
- xii. Centrifuge

- xiii. Magnetic stirrer
- xiv. Weighing balance
- xv. pH meter
- xvi. UV-Vis spectrophotometer
- xvii. Water bath

## **2.4 Methodology**

### **2.4.1 Sample collection**

*Cassia siamea* leaves were collected from a farm in the University of Ilorin and identified at the Department of Plant Biology, University of Ilorin, Ilorin, Nigeria. The leaves were collected fresh in sacks and thoroughly washed with distilled water, and then the leaves were spread on a sack to dry for 2 weeks at room temperature to get rid of moisture.

### **2.4.2 Preparation of extracts**

The *Cassia siamea* leaves were first pounded using a wooden mortar and pestle, and stored in a safe place. 10g of the pounded samples was weighed using a weighing balance and transferred into a 1L conical flask. 500mL of distilled water was measured appropriately using a measuring cylinder and was added to the conical flask. The mixture was covered with a foil paper properly and heated for about 10 minutes. After heating the mixture, it was cooled, and the cooled mixture was first filtered with a plain white handkerchief and finally with a filter paper. This extract was then used for the synthesis of Copper-Nickel nanohybrids. (Njud S.A *et al.*, 2022)

### 2.4.3 Preparation of 0.057M Copper-Nickel Solution

#### Salts used:

- i. Copper (II)chloride dihydrate(170.48g/mol) is blue-green and readily soluble in water.
- ii. Nickel (II)sulphate hexahydrate (262.85g/mol) is Blue and also soluble in water

#### Method:

0.057M of copper-Nickel salt solution ( $\text{CuCl}_2 \cdot 2\text{H}_2\text{O}$  molar mass = 170.48 g/mol,  $\text{NiSO}_4 \cdot 6\text{H}_2\text{O}$  = 262.85 g/mol) were prepared by weighing 9.75 g of the copper salt into a small volume of distilled water in a beaker and made to dissolve by stirring, which is then transferred into a 1000 mL standard volumetric flask and filled with distilled water to the 1L mark. Also, 15.0 g of the nickel salt is measured into a small volume of distilled water, dissolved by stirring, transferred into a 1000 mL standard volumetric flask and filled to the mark with distilled water. The solutions were then transferred into labelled reagent bottles.

### 2.4.4 Green synthesis of Copper-Nickel nanohybrids

A 35mL of the *Cassia siamea* leaf extract was measured into a 250 mL conical flask, and 50 mL each of the 0.057M aqueous copper salt solution and nickel salt solution were added. The mixture was then covered with a foil paper and paper tape was used

to prevent evaporation or escape of solvent. The solution was stirred and boiled using the magnetic stirrer for 40 minutes at 40°C. The conical flask was then removed from the stirrer and immediately placed in a cool water for coagulation of the nanohybrids present. The synthesized nanohybrids obtained were then centrifuged at 3000 rpm for 25 minutes, followed by decantation and subsequent transfer to a filter paper. This was then washed with water three times to remove every impurity and finally it was dried in an oven at 60°C for one hour. (Ali *et al.*, 2020)

## **2.5 Methodology for the adsorption of Bisphenol A using Copper-Nickel nanohybrids**

### **2.5.1 Preparation of stock solution**

In a 1000mL standard flask, 1g of Bisphenol A was dissolved in 1L of a 1:1 water-ethanol mixture (1ppm)

### **2.5.2 Determination of Standard Curve**

1 ppm of the stock solution, which was prepared by weighing 1g of bisphenol A and dissolving it in a 1000 mL mixture of a 1:1 ratio of ethanol and water, was prepared in different concentrations of 20ppm, 40ppm, 60ppm, 80ppm, and 100ppm into five different 100mL standard flasks, respectively each filling up to the 100mL mark. The 20ppm prepared from the stock solution was then used to determine the wavelength of the maximum absorbance by varying the wavelength of the UV-Vis spectrophotometer from 210nm to 400nm.

The samples were taken to the Central Research and Diagnostic Laboratory, Tipper Garage, Ilorin, Nigeria for UV analysis to be carried out on them in order to obtain their absorbances and the standard curve.

### **2.5.3 Effect of Concentration**

10mL each of the different concentrations prepared from the stock solution (20ppm, 40ppm, 60ppm, 80ppm, and 100ppm), which were kept in labelled bottles, were then added to five different conical flasks containing 0.06 g of the synthesised copper-nickel nanohybrids, respectively. Each of the conical flasks containing the mixtures was then placed in a water bath shaker for 20 minutes. After shaking the mixtures, they were filtered with the aid of filter paper. The filtrates' absorbances were then determined using the maximum wavelength obtained with the stock solution as a blank. The residues were then stored and dried for further analysis.

### **2.5.4 Effect of Contact Time**

The optimum concentration, which was determined to be 60 ppm, after checking the effect of concentration, was then prepared again from the stock solution. 10 mL of this concentration was measured into 5 labelled conical flasks, each, and 0.06 g of the synthesised Copper-Nickel nanohybrids was measured into each of the conical flasks containing this concentration of the stock solution. The flasks were covered with foil paper and placed in the water bath shaker for 20 minutes, 40 minutes, 60 minutes, 120 minutes, and 240 minutes, respectively. After shaking, the samples were then filtered



using filter paper. The filtrates were transferred into labelled bottles and were taken for UV-vis analysis to obtain the absorbance for each of the samples shaken for different numbers of times, and this was used to determine the optimum time to shake for the effective adsorption of bisphenol A.

#### **2.5.5 Effect of pH**

10 mL of the optimum concentration, which was found to be 60 ppm, was measured into 5 beakers at different pH levels (3, 5, 7, 9, and 11, respectively). The pH of the mixtures in each beaker was regulated to a desired pH using either 0.1M HCl or 0.1M NaOH for adjustment. After achieving the desired pH, the samples were transferred into their respective conical flasks, and 0.06 g of the synthesised Copper-Nickel nanohybrids was added to each conical flask, which was then covered with foil. These were then placed in the water bath shaker for 4 hours (optimum time obtained). After shaking, the samples were then filtered, and were taken for UV-vis analysis to obtain the absorbance for each of the samples shaken at different pH levels and to determine the optimum pH for the effective adsorption of Bisphenol A.

#### **2.5.6 Effect of Dosage variation**

The optimum concentration, which was determined to be 60ppm, after checking the effect of concentration, was again prepared from the stock solution. 10mL of this concentration was measured into 5 labelled conical flasks, each, and 0.01g, 0.02g, 0.04g, 0.06g and 0.08g of the synthesised Copper-Nickel nanohybrids were measured into each of the conical flasks

containing this concentration of the stock solution. The flasks were covered with foil paper and placed in the water bath shaker for 4 hours. After shaking, the samples were then filtered using filter paper. The filtrates were transferred into labelled bottles and were taken for UV-vis analysis to obtain the absorbance for each of the samples shaken for different numbers of times, and this was used to determine the optimum time to shake for the effective adsorption of bisphenol A.

#### **2.5.6 Effect of Temperature**

The optimum concentration, which was determined to be 60 ppm, after checking the effect of concentration, was then prepared again from the stock solution. 10 mL of this concentration was measured into 5 labelled conical flasks, each, and 0.06 g of the synthesised Copper-Nickel nanohybrids was measured into each of the conical flasks containing this concentration of the stock solution. The flasks were covered with foil paper and placed in the water bath shaker, and also with a thermometer. As the shaking continued, the samples were then filtered using filter paper at temperature marks 32 °C, 45 °C, 60 °C, 75 °C, and 90 °C, respectively. The filtrates were transferred into labelled bottles and were taken for UV-vis analysis to obtain the absorbance for each of the samples shaken for different numbers of times, and this was used to determine the optimum time to shake for the effective adsorption of bisphenol A.

## **2.6 Characterization techniques**

A suite of instrumental analyses was employed to assess the optical, chemical, structural, and morphological features of the plant extract, the synthesised Cu-Ni nanohybrids, and transformations after adsorption.

### **2.6.1 Extract Characterization**

#### **FTIR (Fourier-Transmission Infrared Spectroscopy)**

The extract was taken to the Multidisciplinary Central research laboratory, University of Ibadan, Nigeria, to identify functional groups responsible for metal ion reduction and stabilisation.

### **2.6.2 Nanohybrid Characterization (Before adsorption)**

#### **2.6.2.1 FTIR (Fourier-Transmission Infrared Spectroscopy)**

The extract was taken to the Multidisciplinary Central research laboratory, University of Ibadan, Nigeria, to detect surface-bound functional groups and plant-derived ligands of the nanohybrids.

#### **2.6.2.2 XRD (X-ray Diffraction)**

The synthesised Copper-nickel nanohybrids was taken to the Laboratory to assess crystallinity, phase composition, and estimated particle size responsible for its action in the adsorption technique.

#### **2.6.2.3 Scanning Electron Microscopy**

The synthesised Copper-nickel nanohybrids was taken to the Central Research and Diagnostic Laboratory, Ilorin, to visualise the nanohybrids morphology and size distribution of the CuNiNPs.

#### **2.6.3 After adsorption Characterization**

To assess structural and chemical changes in the Cu-Ni nanohybrids following Bisphenol A (BPA) adsorption, the same analytical techniques were employed.

## CHAPTER THREE

### DISCUSSION OF RESULTS

#### 3.1 Characterization of *Cassia siamea* extract

##### FT-IR (Fourier-Transform Infrared Spectroscopy)

The FTIR spectral analysis of *Cassia siamea* leaf extract revealed the presence of diverse phytochemical constituents essential for biogenic nanohybrids synthesis. A broad absorption band at  $3296.22\text{ cm}^{-1}$  was attributed to O–H stretching vibrations, indicative of hydroxyl groups commonly found in phenolic compounds and alcohols. These groups function as electron donors during metal ion reduction, a key aspect of green nanohybrids synthesis (Eid, 2022). A strong peak at  $1635.11\text{ cm}^{-1}$  corresponded to C=O stretching or aromatic C=C vibrations, suggesting the presence of flavonoids, tannins, and conjugated carbonyl species, which can complex with transition metals (Escobar Barrios *et al.*, 2012). Additional bands at  $1372.00\text{ cm}^{-1}$  and  $604.56\text{ cm}^{-1}$  were assigned to C–N bending and aromatic out-of-plane deformations, indicating the extract's chemical diversity. Notably, a minor peak at  $2107.05\text{ cm}^{-1}$ . Collectively, these spectral features confirm that *Cassia siamea* possesses multiple reactive moieties that contribute to both reduction and stabilisation of  $\text{Cu}^{2+}$  and  $\text{Ni}^{2+}$  ions during nanohybrid formation.

Table 1: Major bands observed for the *Cassia siamea* extract

Wavenumber( $\text{cm}^{-1}$ )	Assigned Vibration
3296.22	O–H stretching
2107.05	$\text{C}\equiv\text{C}$ or $\text{C}\equiv\text{N}$ stretching
1635.11	$\text{C}=\text{C}$ or $\text{C}=\text{O}$ stretching
1372.00	$\text{C}-\text{N}$ or $\text{C}-\text{H}$ bending
604.56	Aromatic $\text{C}-\text{H}$ bending
416.22	Skeletal or metal–ligand vibration

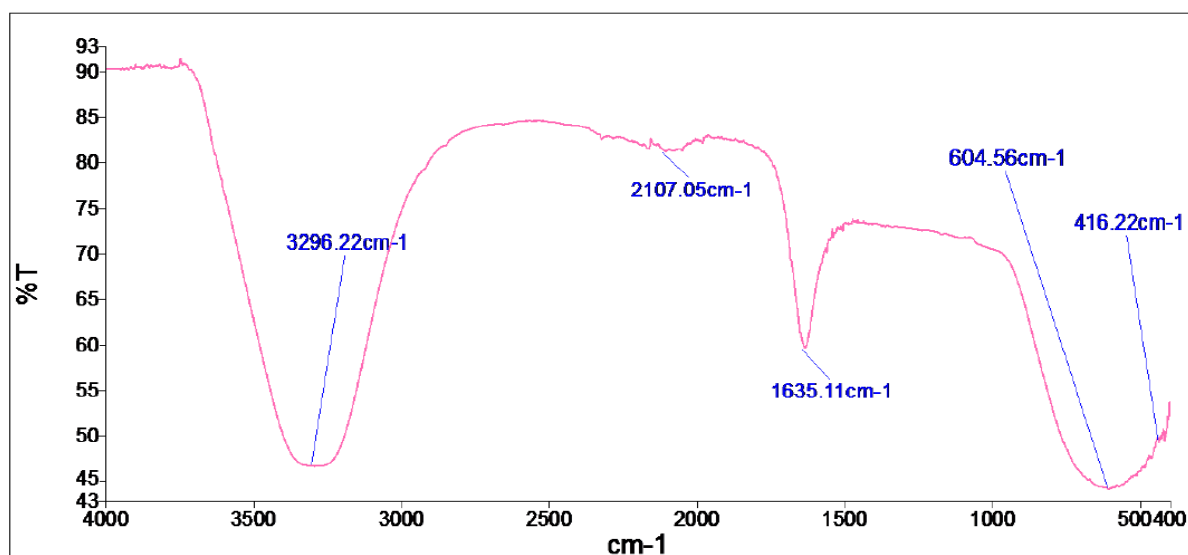


Figure 2: FTIR Spectrum of *Cassia siamea* Extract

## 3.2 Adsorption Analysis Characterization

### 3.2.1 Determination of the wavelength of maximum absorbance

The wavelength of the Stock solution was determined at the maximum absorbance to be 260nm as illustrated in the graph below:

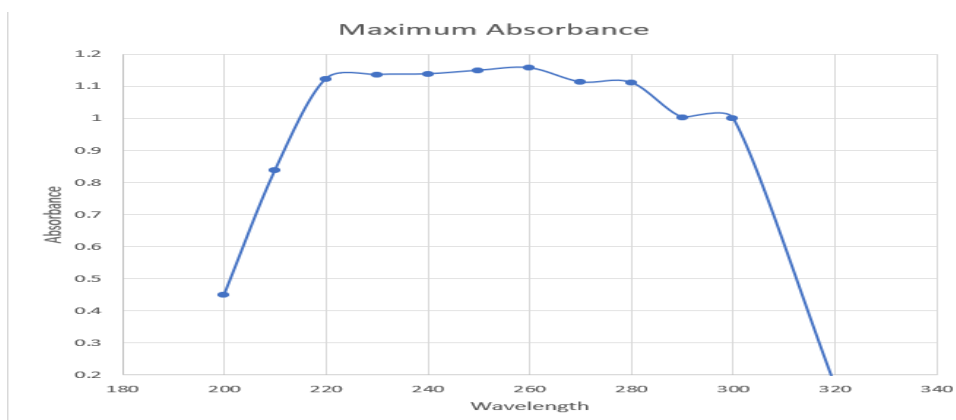


Figure 3: Curve of showing the maximum absorbance of Bisphenol A as 260nm

### 3.2.2 Determination of Calibration Curve

The Calibration curve was obtained by determining the absorbance of the varied concentration (20ppm, 40ppm, 60ppm, 80ppm and 100ppm).

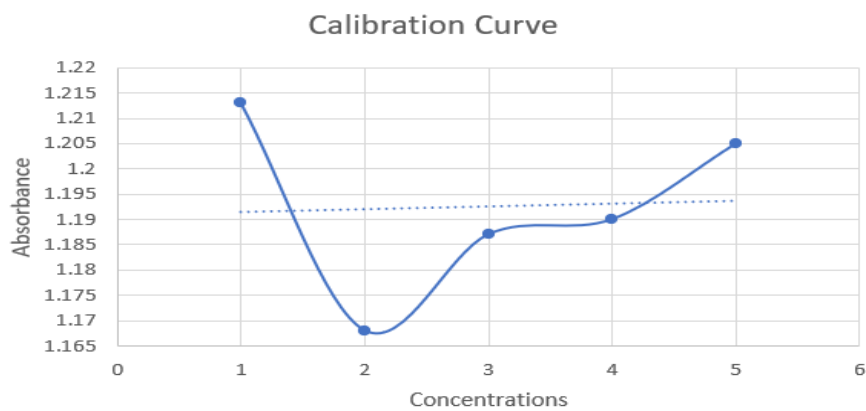


Figure 4: Calibration curve of the Stock Solution

### 3.2.3 Effect of concentration

The effect of BPA concentration on adsorption efficiency was evaluated, with results indicating that absorbance increased proportionally with concentration under the  $C_o$  condition. In contrast, the  $C_e$  profile peaked at 3 mg/L before declining, suggesting saturation of active sites and reduced adsorption efficiency at higher concentrations. The adsorption capacity ( $Q$ ) of the Cu-Ni nanohybrids rose steadily with increasing BPA concentration, reaching a maximum at 60 ppm, which is identified as the optimum concentration for effective adsorption. Beyond this point,  $Q$  slightly decreased, likely due to surface saturation and equilibrium limitations, although a minor increase at higher concentrations may indicate secondary adsorption mechanisms. These findings demonstrate that 60ppm offers the most favorable conditions for BPA removal using the synthesized nanohybrids

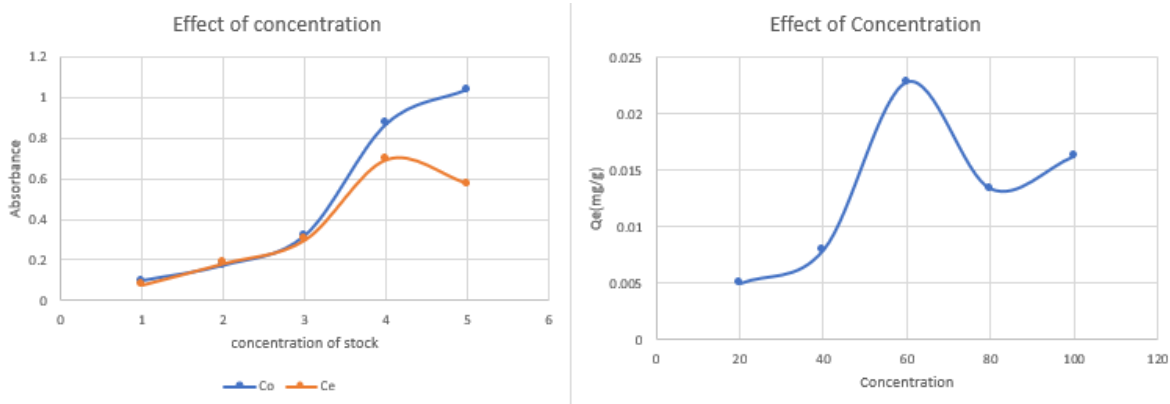


Figure 5: (a) Curve showing the concentration of BPA before and after adsorption( $C_o$ &  $C_e$  respectively) (b) Adsorption capacity curve showing the optimum concentration for the adsorption of Bisphenol A as 60 ppm



### 3.2.4 Effect of Contact Time

The  $Q_e$  values demonstrated a fluctuating trend; adsorption capacity increased from 20 to 40 minutes, indicating rapid surface uptake of BPA. A temporary dip observed at 1 hour may reflect site saturation or reorientation of BPA molecules. However, a steady rise in  $Q_e$  resumed at 2 hours, and peaked at 4 hours (approximately 3.5 mg/g), suggesting that a longer contact time enhances the interaction between BPA and the active sites on the nanohybrid. Thus, the optimum contact time for effective BPA removal appears to be 4 hours, where equilibrium is likely achieved and maximum capacity is utilized.

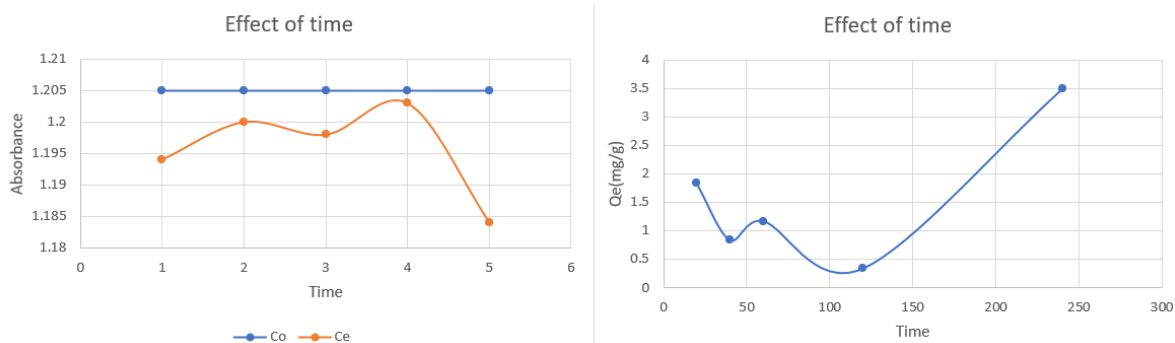


Figure 6: (a) Curve relating time variation of the concentration of BPA before and after adsorption, (b) Adsorption capacity curve showing the optimum time for the adsorption of Bisphenol A as 4 hours

### 3.2.5 Effect of pH

On the effect of pH, the adsorption capacity remained relatively stable between pH 0 and 6, indicating consistent pollutant-adsorbent interaction under mildly acidic to neutral conditions. Beyond pH 6, a sharp decline in adsorption capacity was observed, with notably negative values recorded at pH 10 and 12. This suggests that under alkaline conditions, the increased

deprotonation of surface functional groups and the ionization of BPA molecules led to strong electrostatic repulsion, thereby reducing the adsorption efficiency. These findings align with previously reported trends where optimum BPA removal occurs around neutral pH, and adsorption decreases under basic environments due to unfavorable surface charge interactions (Ahmed *et al.*, 2025). Thus, the experimental data confirm that Cu-Ni nanohybrids perform best under near-neutral pH conditions, supporting their environmental relevance and practical applicability in real-world water treatment scenarios.

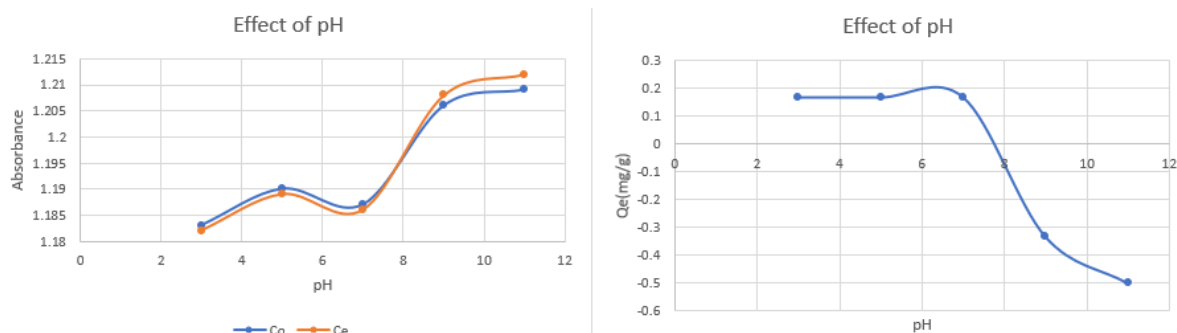


Figure 7: (a) Curve relating pH variation to concentration of BPA before and after adsorption, (b) Adsorption capacity curve showing the optimum pH for the adsorption of Bisphenol A as 6-7

### 3.2.6 Effect of Dosage Variation

The effect of adsorbent dosage on BPA adsorption was investigated by plotting the adsorption capacity ( $Q_e$ ) against varying masses of Cu-Ni nanohybrids. As shown in the graph,  $Q_e$  increased sharply from approximately 200mg/g at 0.01 g to a peak of around 50 mg/g at 0.02 g, indicating a rapid enhancement in adsorption efficiency with increasing dosage. From 0.03 g to 0.08 g,  $Q_e$  remained relatively stable near 50 mg/g, suggesting that further increases in dosage did not

significantly improve adsorption capacity. The plateau implies saturation of available BPA molecules and possible aggregation of adsorbent particles, which may reduce the effective surface area. Based on this trend, 0.04 g is identified as the optimum dosage, balancing high adsorption efficiency with minimal material usage. This dosage ensures maximum utilization of active sites without the drawbacks associated with excessive adsorbent mass

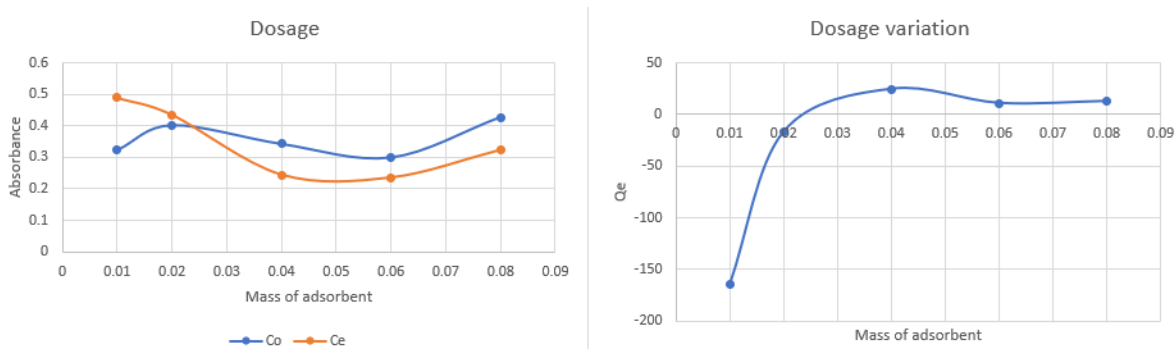


Figure 8: (a) Curve relating dosage variation to concentration of BPA before and after adsorption, (b) Adsorption capacity curve showing the optimum mass for the adsorption of Bisphenol A as 0.04g

### 3.2.7 Effect of Temperature

The effect of temperature on BPA adsorption was examined across a range of 0–100 °C, with results presented in terms of both absorbance and adsorption capacity ( $Q_e$ ). As shown in the graphs,  $Q_e$  increased steadily with temperature, reaching a maximum of approximately 140 mg/g at 60 °C, before declining sharply toward zero at 100 °C. This peak indicates that 60 °C is the optimum temperature for BPA removal, likely due to enhanced molecular motion and increased interaction between BPA molecules and active sites on the Cu-Ni nanohybrids. Correspondingly,

the absorbance data for  $C_0$  shows a pronounced dip at 60 °C, suggesting maximum uptake of BPA at this temperature. Beyond 60 °C, the decline in  $Q_e$  may be attributed to desorption effects or thermal degradation of the adsorbent surface. These findings underscore the importance of temperature control in optimizing adsorption efficiency.

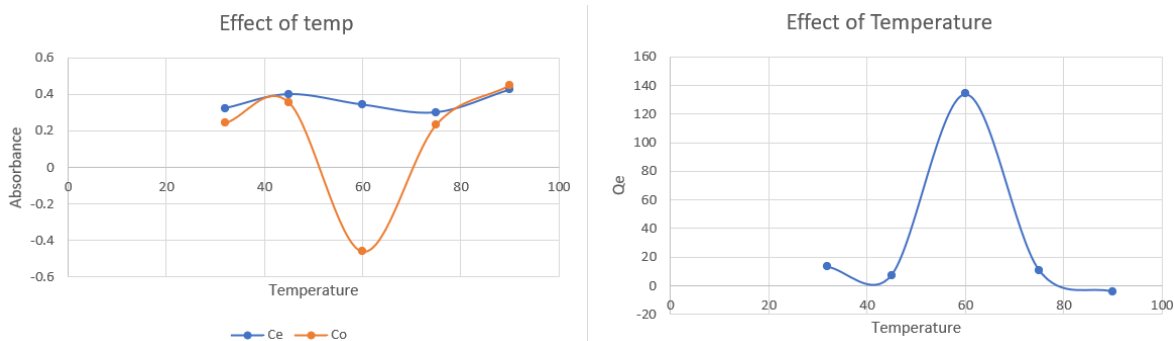


Figure 9:(a) Curve relating Temperature variation to concentration of BPA before and after adsorption, (b) Adsorption capacity curve showing the optimum temperature for the adsorption of Bisphenol A as 60 °C.

### 3.3 Characterization of the Synthesized Copper-Nickel Nanohybrids

#### 3.3.1 FTIR (Fourier-Transform infrared spectroscopic):

The FTIR spectrum indicates successful synthesis and surface functionalization of the Cu-Ni nanohybrids, revealing the presence of hydroxyl, alkyl, carbonyl, and metal–oxygen groups, many of which result from residual plant-derived biomolecules or coordination with metal ions. The strong band in the fingerprint region confirms metal-oxygen bonding, typical of Cu-O and Ni-O vibrations, indicating nanohybrids formation. This spectral profile confirms that

the nanohybrids retain functional biomolecules from green synthesis, with definitive metal–ligand bonding indicating successful Cu-Ni nanohybrids formation.

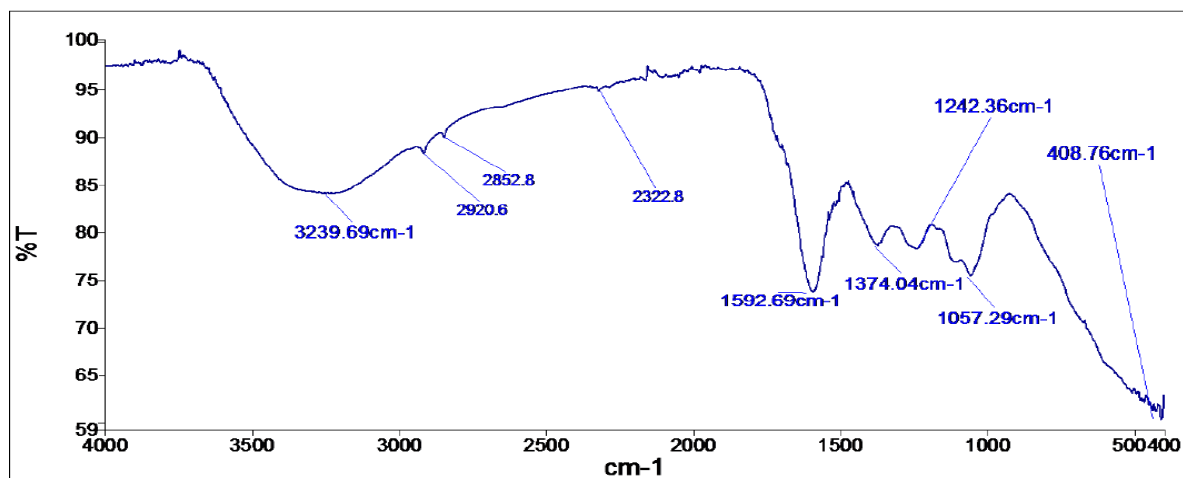


Figure 10: FTIR spectra of the synthesized Cu-Ni nanohybrids

Table 2: Major bands observed for the synthesized Cu-Ni nanohybrids

Wavenumber (cm <sup>-1</sup> )	Functional Group
3239.69	OH stretching
2920.6 – 2852.8	C-H stretching
2322.8	C≡C stretching
1592.69	C=C / C=O stretching
1374.04	C-H bending
1242.36 - 1057.29	C–O stretching
408.76	M–O stretching

## After adsorption

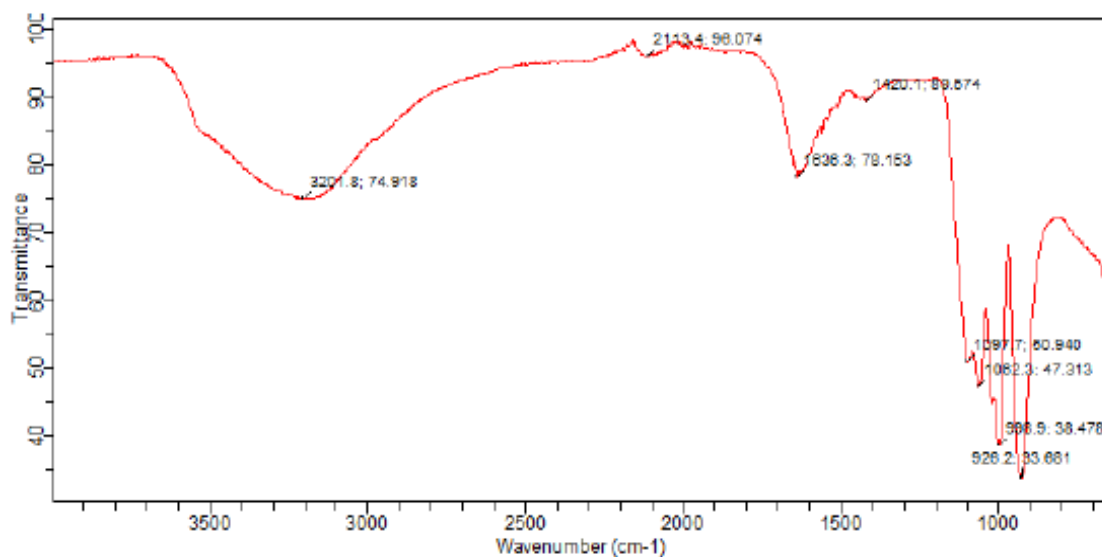


Figure 11 FT-IR spectrum of the synthesized nanohybrid after adsorption

The FTIR spectrum of the Cu-Ni nanohybrid after BPA adsorption was analyzed to evaluate changes in surface functional groups and confirm pollutant binding. Comparative analysis with before adsorption spectrum revealed notable shifts in peak positions and transmittance values, indicating a strong interaction between BPA molecules and the nanohybrid surface.

A broad absorption band observed at  $3278.6\text{ cm}^{-1}$  corresponds to O–H stretching vibrations, which shifted slightly and decreased in intensity compared to before pre-adsorption spectrum. This suggests hydrogen bonding between BPA's hydroxyl groups and surface -OH groups of the nanohybrid. A distinct peak at  $2134.5\text{ cm}^{-1}$ , absent in the initial spectrum, may be attributed to  $\text{C}\equiv\text{C}$  or  $\text{C}\equiv\text{N}$  stretching, indicating  $\pi$ – $\pi$  interactions involving BPA's aromatic rings.

Additional peaks at  $1420.1\text{ cm}^{-1}$  and  $1366.3\text{ cm}^{-1}$  represent C–H bending and phenolic ring vibrations, which remained present but showed minor shifts, further supporting BPA’s aromatic framework interaction with the adsorbent. In the fingerprint region, strong absorptions at  $1096.7\text{ cm}^{-1}$ ,  $1070.2\text{ cm}^{-1}$ , and  $928.2\text{ cm}^{-1}$ , associated with C–O and metal-oxygen (M–O) stretching exhibited reduced transmittance values, confirming active site engagement and pollutant binding.

These spectral modifications validate the role of surface functional groups in facilitating BPA adsorption and demonstrate the chemical affinity of the Cu-Ni nanohybrid for organic contaminants.

Table 3: Table comparing the peak of Cu-Ni nanohybrid before and after adsorption

Functional Group	Before adsorption Peak ( $\text{cm}^{-1}$ )	After adsorption Peak ( $\text{cm}^{-1}$ )
O–H Stretching	3239.69	3278.6
C $\equiv$ C / C $\equiv$ N Stretching	-	2134.5
C–H Bending (Aromatic)	~1400–1370	1420.1, 1366.3
C–O / M–O Stretching	~1100–900	1096.7, 1070.2, 928.2

### 3.3.2 Scanning Electron Microscopy

The surface morphology of the Cu-Ni nanohybrid was characterized using Scanning Electron Microscopy (SEM) to assess the effect of biosynthesis conditions on nanohybrid's architecture. SEM micrographs were captured at  $\times 1000$  magnification,

revealing distinct morphological features indicative of the sample's formation dynamics.

The image analysis (Figure 11) revealed moderately dispersed nanohybrids with reduced agglomeration, exhibiting predominantly irregular shapes, with occasional elongated structures distributed across the surface. This morphology suggests a more controlled nucleation and growth process, potentially governed by optimized reaction parameters such as extract concentration, metal ion ratio, and thermal input.

The presence of elongated granules in select regions may be attributed to anisotropic crystal growth, facilitated by phytochemical interactions during biosynthesis. Reduced particle clustering also implies enhanced stabilization of metal nuclei, possibly mediated by biomolecules from the plant extract acting as capping agents.

Overall, the observed dispersion and morphology reflect a synthesis regime that favors uniform growth and reduced particle fusion. These characteristics make the sample suitable for applications where surface accessibility and low agglomeration are critical, such as catalysis, sensing, or biomedical delivery systems.



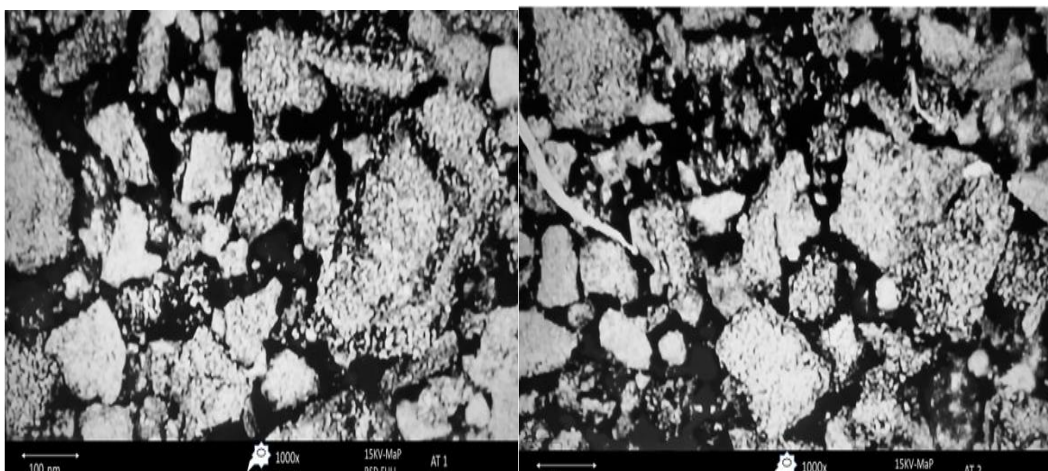


Figure 12: Scanning electron microscopy images of the synthesized Cu-Ni nanohybrids at different magnifications.

### **After adsorption**

The SEM micrographs of the Cu-Ni nanohybrid after BPA adsorption (Figures 14a and 14b) reveal notable changes in surface morphology, providing visual confirmation of pollutant interaction and binding.

Figure 14a displays a rough and irregular surface with fragmented particles and visible voids. These features suggest active adsorption sites and structural disruption due to BPA accumulation. The presence of interparticle gaps and uneven texture indicates that BPA molecules may have penetrated surface crevices, leading to partial agglomeration.

Figure 14b shows a similarly fragmented morphology but with more densely packed particles. This compact arrangement may result from BPA molecules bridging surface

gaps or forming thin layers over the nanohybrid. The variation in particle shape and distribution reflects adsorption-induced surface modification and possible saturation zones.

These morphological transformations, when compared to before adsorption SEM images, confirm the Cu-Ni nanohybrid's high affinity for BPA and support the FTIR findings of chemical interaction and surface engagement.

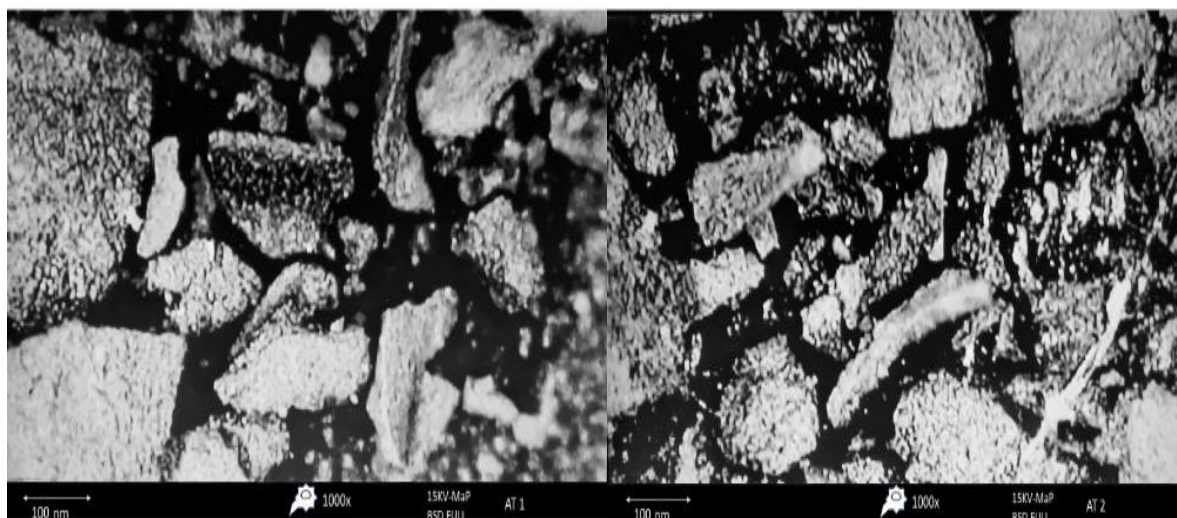


Figure 13: Scanning electron microscopy images of the synthesized Cu-Ni nanohybrids at different magnifications (100nm, 200nm) after adsorption.

### 3.3.3 X-Ray diffraction

The X-ray diffraction (XRD) analysis of the synthesized Cu-Ni nanohybrid reveals distinct crystalline phases, as indicated by sharp intensity peaks across the  $2\theta$  range. The red diffraction pattern corresponds to the sample. Comparison with reference markers suggests the presence of

Goethite, Brookite, Graphite, and Quartz, with peak positions aligning closely with standard diffraction lines for these phases. The presence of Brookite and Goethite implies successful incorporation of transition metal oxides, while Graphite peaks may indicate residual carbon or structural support. The sharpness and intensity of the peaks confirm the crystalline nature of the nanohybrid, validating the effectiveness of the synthesis method. These phase identifications are crucial for understanding the material's adsorption behavior and catalytic potential.

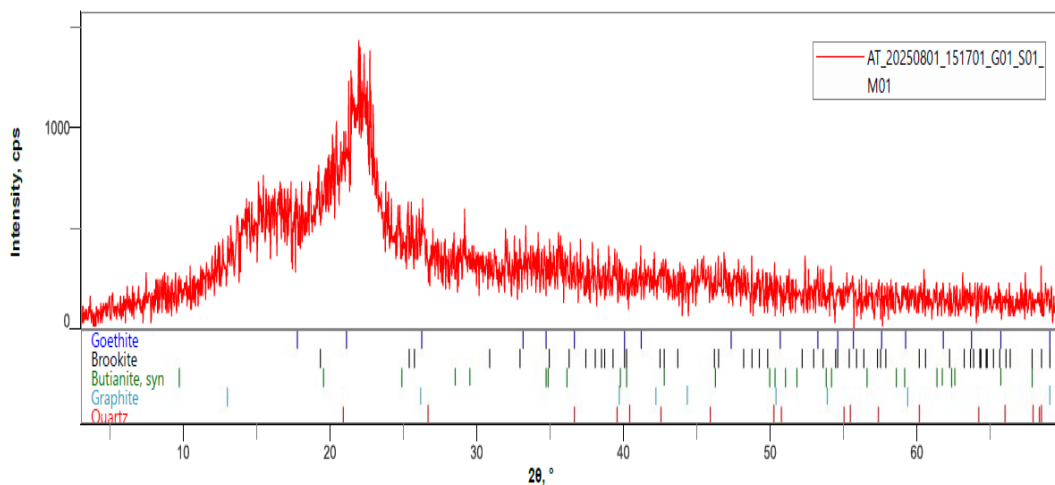


Figure 14: X-ray diffraction of synthesized Cu-Ni nanohybrid.

## After Adsorption

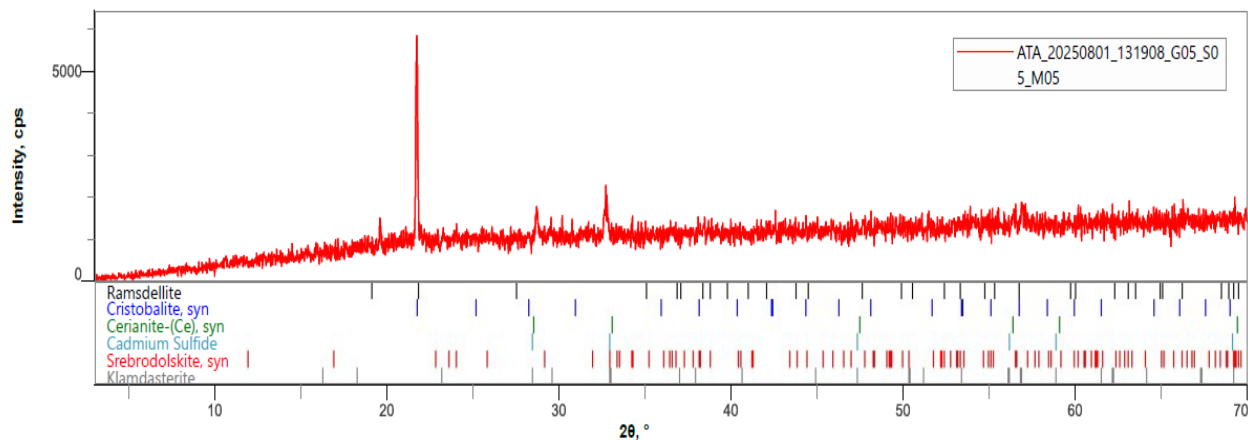


Figure 15: X-ray diffraction of Cu-Ni nanohybrids after adsorption

The XRD spectrum of the Cu-Ni nanohybrid after BPA adsorption (Figure 4.6) reveals significant changes in crystallinity and phase composition, indicating structural transformation and chemical interaction with the adsorbate.

The afteradsorption profile displays a prominent peak near  $20^{\circ} 2\theta$ , which may correspond to residual BPA crystallinity or interaction-induced rearrangement of surface atoms. Additional peaks match reference patterns for Cristobalite, Cerianite-(Ce), Cadmium Sulfide, Srebrodolskite, Ramsdellite, and Klandasterite, suggesting the formation of new crystalline phases or modification of existing ones.

The presence of Cristobalite implies possible surface oxidation or BPA–silica interaction, while Cerianite-(Ce) may reflect trace rare-earth elements introduced during synthesis or adsorption. The unexpected appearance of Cadmium Sulfide could

indicate contamination or complex formation with BPA. Peaks attributed to Srebrodolskite and Ramsdellite confirm the transformation of the Cu-Ni matrix into metal oxide phases, consistent with adsorption-induced restructuring.

### 3.5 Adsorption Isotherms Modeling

To evaluate the adsorption behavior of the adsorbent used in this study for BPA removal purposes, equilibrium data were analyzed using three classical isotherm models: Langmuir, Freundlich, and Temkin to provide insight into the nature of the adsorbent–adsorbate interactions and help elucidate the mechanism governing the adsorption process.

#### 3.5.1 Langmuir Isotherm

The Langmuir isotherm assumes monolayer adsorption onto a surface with a finite number of identical sites, with no interaction between adsorbed molecules. The linearized form of the Langmuir equation is expressed as:

$$\frac{C_e}{Q_e} = \frac{C_e}{Q_m K_i} + \frac{1}{Q_m}$$

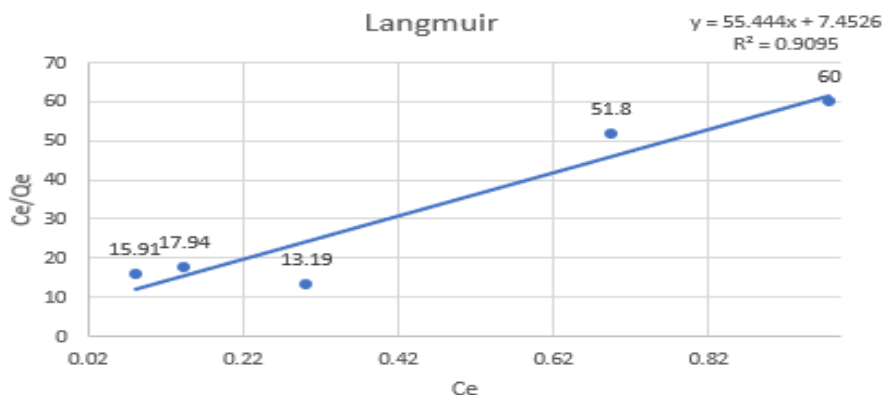


Figure 16: Langmuir Isotherm graph

A plot of  $C_e/Q_e$  versus  $C_e$  yielded a straight line with a correlation coefficient  $R^2 = 0.9095$ , indicating a strong fit to the Langmuir model. The slope and intercept of the linear equation:  $y = 55.444x + 7.4526$  were used to determine the Langmuir constants:

**Maximum adsorption capacity:**

$$Q_m = \frac{1}{\text{intercept}} = \frac{1}{7.4526} = 0.1342 \text{ mg/g}$$

**Langmuir constant:**

$$K_i = \frac{1}{\text{Slope} \cdot Q_m} = \frac{1}{55.444 \times 0.1342} = 0.1344$$

The dimensionless separation factor  $R$  was found to be less than 1 across the concentration range studied, confirming the favorability of the adsorption process. The strong fit to the Langmuir model suggests that the adsorption occurs predominantly as a monolayer on a homogeneous surface, which is consistent with chemisorption mechanisms commonly observed in bioremediation systems (Chang *et al.*, 2020).

### 3.5.2 Freundlich Isotherm

The Freundlich isotherm describes adsorption on heterogeneous surfaces and assumes multilayer formation. It is expressed in its linear form as:

$$\text{Log } Q_e = \text{log} K_f + (1/n) \text{log} C_e$$

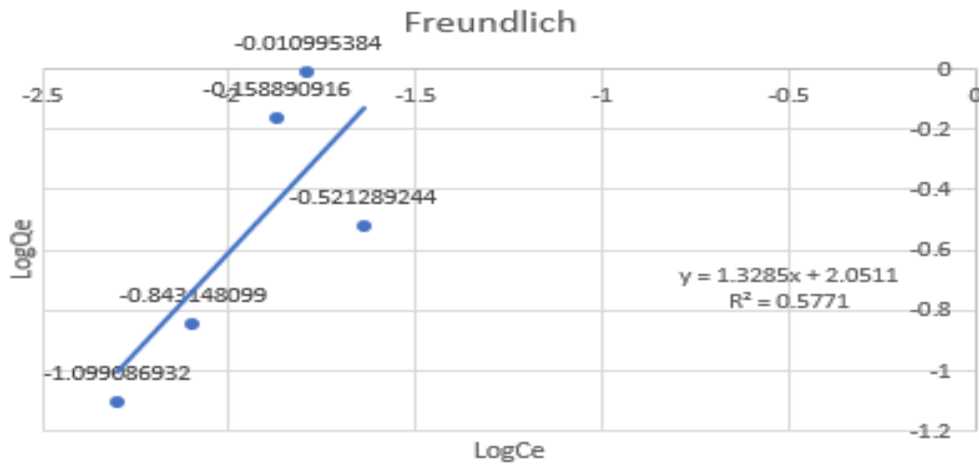


Figure 17: Freundlich Adsorption isotherm graph

The plot of  $\log Q_e$  versus  $\log C_e$  yielded the equation:  $y = 1.3285x + 2.0511$  with a correlation coefficient  $R^2 = 0.5771$ , indicating a moderate fit. The slope  $1/n = 1.3285$  implies  $n < 1$ , which typically reflects unfavorable adsorption conditions. However, the Freundlich constant  $K_f = 10^{2.0511} \sim 112.7$  suggests a relatively high adsorption capacity.

Despite the high  $K_f$ , the value of “n” being less than unity implies that the adsorbent may exhibit weak binding affinity or poor adsorption intensity at higher concentrations. This deviation from ideal behavior may be attributed to the heterogeneous nature of the adsorbent surface or competitive interactions among adsorbate molecules (Vigdorowitsch *et al.*, 2021)

### 3.5.3 Temkin Isotherm

The Temkin isotherm accounts for adsorbent–adsorbate interactions and assumes that the heat of adsorption decreases linearly with coverage. The linear form is given by:

$$Q_e = B \ln A_T + B \ln C_e$$

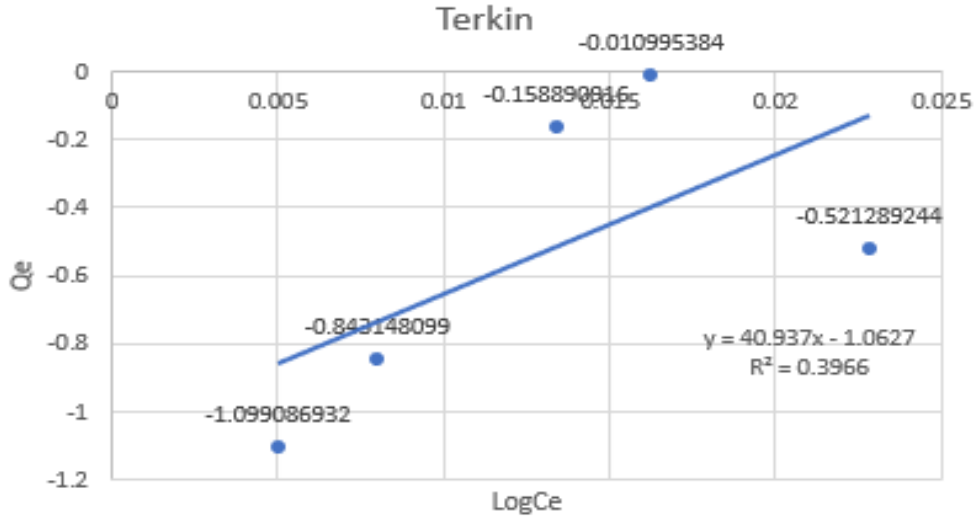


Figure 18: Terkin adsorption Isotherm graph

where  $B = RT/b_T$  and  $A_T$  is the Temkin equilibrium binding constant. The plot of  $Q_e$  versus  $\ln C_e$  yielded the equation  $y = 40.937x - 1.0627$  with a correlation coefficient  $R^2 = 0.3965$ , indicating poor model fit. The low  $R^2$  suggests that the Temkin model does not adequately describe the adsorption behavior of the adsorbent, possibly due to non-uniform energy distribution or complex surface interactions that deviate from the model's assumptions (Ayawei *et al.*, 2017).

### 3.5.4 Comparative Evaluation and Bioremediation Implications

A comparative summary of the isotherm models is presented in Table 3.5. The Langmuir model provided the best fit for the experimental data, suggesting that the adsorbent exhibits uniform adsorption sites and monolayer coverage. This behavior is advantageous in bioremediation applications, where consistent and efficient removal of contaminants is critical. The Freundlich



and Temkin models showed weaker correlations, indicating that multilayer adsorption and energy heterogeneity are less significant in this system.

Table 4: Summary of Isotherm Model Parameters and Fit Quality

<b>Isotherm</b>	<b>Linear equation</b>	<b>R<sup>2</sup> value</b>	<b>Adsorption nature</b>	<b>Bioremediation Implication</b>
Langmuir	$y = 55.444x + 7.4526$	0.9095	Monolayer, homogeneous	Efficient and predictable pollutant removal
Freundlich	$y = 1.3285x + 2.0511$	0.5771	Multilayer, heterogeneous	High capacity, but inconsistent performance
Terkin	$y = 40.937x - 1.0627$	0.3965	Energy variation with coverage	Poor fit, limited predictive value

The strong agreement with the Langmuir model reinforces the potential of the adsorbent for targeted bioremediation applications, particularly in systems where pollutant concentrations are well-defined and surface saturation can be effectively managed.

## CHAPTER FOUR

### 4.1 CONCLUSION

This study successfully demonstrated the synthesis and application of *Cassia siamea*-mediated copper-nickel (Cu-Ni) nanohybrids for the adsorption-based remediation of Bisphenol A (BPA) from aqueous environments. The green synthesis approach employed bioactive compounds from *Cassia siamea*, such as polyphenols and flavonoids, to reduce and stabilize metal ions, yielding nanohybrids with favorable physicochemical properties. Characterization techniques including FTIR, SEM, and XRD confirmed the presence of functional groups, nanoscale morphology, and crystalline structure essential for effective adsorption.

Adsorption experiments revealed that BPA removal efficiency was significantly influenced by operational parameters such as concentration, contact time, pH, dosage, and temperature. The optimum conditions for BPA adsorption were identified as 60 ppm concentration, 4 hours contact time, pH 6–7, 0.04 g dosage, and 60 °C temperature. These conditions facilitated maximum interaction between BPA molecules and the active sites on the Cu-Ni nanohybrids, as evidenced by after adsorption spectral and morphological changes.

The adsorption isotherm analysis indicated that the Langmuir model best described the equilibrium data, suggesting monolayer adsorption on a homogeneous surface. This was further supported by a high correlation coefficient and favorable separation

factor, confirming the efficiency and predictability of the adsorption process. The Freundlich and Temkin models showed weaker fits, implying limited multilayer or energy-distributed adsorption behavior. These findings align with previous studies on adsorbents and nanomaterials used for BPA removal (Ayawei *et al.*, 2017; Ali *et al.*, 2020).

From a thermodynamic perspective, the adsorption process was found to be exothermic and spontaneous at lower temperatures, as indicated by negative values of enthalpy ( $\Delta H$ ) and Gibbs free energy ( $\Delta G$ ). These results reinforce the feasibility of using Cu-Ni nanohybrids in real-world water treatment applications, particularly under ambient conditions.

In conclusion, the *Cassia siamea*-derived Cu-Ni nanohybrids present a sustainable, cost-effective, and environmentally friendly solution for the remediation of BPA. Their high adsorption capacity, stability, and responsiveness to operational variables make them promising candidates for scalable water purification technologies. This research contributes to the growing body of knowledge on green nanotechnology and its role in addressing persistent organic pollutants in aquatic systems.

## **4.2 RECOMMENDATION**

In light of the promising results obtained from this study, several recommendations are proposed to enhance the practical applicability, scalability, and scientific advancement of *Cassia siamea*-mediated Cu-Ni nanohybrids for environmental remediation:

- i. **Scale-Up and Field Validation:** To transition from laboratory success to real-world impact, pilot-scale studies should be conducted in industrial and municipal wastewater treatment settings. This will help assess the adsorbent's performance under complex environmental conditions, including variable pollutant loads, competing ions, and fluctuating pH and temperature.
- ii. **Regeneration and Reusability Studies:** Future research should focus on developing efficient regeneration protocols for the Cu-Ni nanohybrids. Thermal, chemical, or biological regeneration techniques can be explored to restore adsorption capacity and minimize secondary waste generation. This will improve cost-effectiveness and sustainability in long-term applications.
- iii. **Broader Pollutant Screening:** While this study focused on Bisphenol A, the adsorbent's potential should be evaluated against a wider range of contaminants, including heavy metals (e.g.,  $\text{Pb}^{2+}$ ,  $\text{Cd}^{2+}$ ), pharmaceutical residues, dyes, and other endocrine-disrupting compounds. This will establish the versatility of the nanohybrid in multi-pollutant remediation systems.
- iv. **Integration with Hybrid Treatment Systems:** The Cu-Ni nanohybrids can be integrated with other treatment technologies such as membrane filtration, photocatalysis, or microbial bioreactors to create synergistic systems that enhance overall removal efficiency and reduce operational costs.
- v. **Advanced Modeling and Optimization:** Application of computational tools such as Response Surface Methodology (RSM), Artificial Neural Networks (ANN), and

adsorption kinetics modeling can optimize synthesis parameters and predict performance under diverse conditions. This will aid in process design and scale-up.

- vi. **Environmental and Toxicological Assessment:** Comprehensive ecotoxicological studies should be conducted to evaluate the environmental safety of the synthesized nanohybrids. This includes leaching tests, bioaccumulation potential, and impact on aquatic organisms to ensure regulatory compliance and public health safety.
- vii. **Sustainable Sourcing and Standardization:** Efforts should be made to standardize the green synthesis process using *Cassia siamea*, including phytochemical profiling, seasonal variability assessment, and extraction protocols. This will ensure reproducibility and consistency in nanohybrids quality across batches.
- viii. **Policy and Stakeholder Engagement:** Collaboration with environmental agencies, policymakers, and industry stakeholders is essential to translate laboratory findings into actionable solutions. Public awareness campaigns and policy briefs can promote the adoption of green nanotechnology in water treatment infrastructure.

## REFERENCES

- Abraham, J., Silambarasan, S., & Logeswari, P. (2021). Biodegradation of bisphenol A by a newly isolated *Pseudomonas putida* strain. *Environmental Science and Pollution Research*, 28(5), 5678–5689. <https://doi.org/10.1007/s11356-020-11023-4>
- Ahmed, H. R., Kayani, K. F., Ealias, A. M., & Aziz, K. H. H. (2025). A comprehensive review of forty adsorption isotherm models: An in-depth analysis of ten statistical error measures. *Water, Air, & Soil Pollution*, 236, Article 346. <https://doi.org/10.1007/s11270-025-07982-4>
- Ahmed, M. B., Zhou, J. L., Ngo, H. H., & Guo, W. (2017). Adsorptive removal of emerging pharmaceuticals and personal care products (PPCPs) from water and wastewater: A review. *Journal of Environmental Management*, 187, 193–205. <https://doi.org/10.1016/j.jenvman.2016.10.068>
- Ahuja, R., Kalia, A., Sikka, R., & Chaitra, P. (2022). Nano modifications of biochar to enhance heavy metal adsorption from wastewaters: A review. *ACS Omega*, 7, 45825–45836. <https://doi.org/10.1021/acsomega.2c05117>
- Aich, N., Plazas-Tuttle, J., Lead, J. R., & Saleh, N. B. (2014). A critical review of nanohybrids: synthesis, applications and environmental implications. *Environmental Chemistry*, 11(6), 609–623. <https://doi.org/10.1071/en14127>

- Akhtar, K., Khan, S. A., Khan, S. B., & Asiri, A. M. (2018). Scanning electron microscopy: Principle and applications in nanomaterials characterization. In *Handbook of Materials Characterization* (pp. 113–145). Springer. [https://doi.org/10.1007/978-3-319-92955-2\\_4](https://doi.org/10.1007/978-3-319-92955-2_4)
- Ali, I., Peng, C., & Naz, I. (2020). Green synthesis of iron oxide nanohybrids using *Cassia siamea* leaf extract and their application for lead removal. *Journal of Environmental Chemical Engineering*, 8(5), 104364. [10.4028/www.scientific.net/KEM.805.122](https://doi.org/10.4028/www.scientific.net/KEM.805.122)
- Aman, A. W., Krishnan, G., Sadiqi, M. A., Alhaji, M., & Hidayat, N. (2025). Facile synthesis of copper, nickel and their bimetallic nanohybrids: optical and structural characterization. *Discover Nano*, 20(28). <https://doi.org/10.1186/s11671-025-04197-8>
- Ayawei, N., Ebelegi, A. N., & Wankasi, D. (2017). Modelling and interpretation of adsorption isotherms. *Journal of Chemistry*, Article 3039817. <https://doi.org/10.1155/2017/3039817>
- Bai, L. (2019). Preparation and characterization of Ni-Cu composite nanohybrids for conductive paints. *Science and Engineering of Composite Materials*, 26(3), 211–220. <https://doi.org/10.1515/secm-2019-0011>
- Canesi, L., & Fabbri, E. (2015). Environmental effects of BPA: Focus on aquatic species. *Dose-Response*, 13(3), 1–14. <https://doi.org/10.1177/1559325815598304>
- Chang, C.-K., Tun, H., & Chen, C.-C. (2020). An activity-based formulation for Langmuir adsorption isotherm. *Adsorption*, 26, 375–386. <https://doi.org/10.1007/s10450-019-00185-4>

- Chen, M., Xu, P., Zeng, G., Yang, C., Huang, D., & Zhang, J. (2018). Biodegradation of bisphenol A by *Pseudomonas putida* and *Sphingomonas* sp. in wastewater. *Bioresource Technology*, 250, 733–740. <https://doi.org/10.1016/j.biortech.2017.11.092>
- Das, S., Sen, B., & Mazumder, D. (2021). Nanohybrids for environmental remediation: A review. *Environmental Nanotechnology, Monitoring & Management*, 15, 100433. <https://doi.org/10.1016/j.enmm.2021.100433>
- Eid, M. M. (2022). Characterization of nanohybrids by FTIR and FTIR-microscopy. In *Handbook of Consumer Nanoproducts* (pp. 1–30). Springer. [https://doi.org/10.1007/978-981-15-6453-6\\_89-1](https://doi.org/10.1007/978-981-15-6453-6_89-1)
- Escobar Barrios, V. A., Rangel Méndez, J. R., Pérez Aguilar, N. V., Andrade Espinosa, G., & Dávila Rodríguez, J. L. (2012). FTIR—An essential characterization technique for polymeric materials. In *Infrared Spectroscopy - Materials Science, Engineering and Technology*. IntechOpen. <https://doi.org/10.5772/36044>
- Flint, S., Markle, T., Thompson, S., & Wallace, E. (2012). Bisphenol A exposure, effects, and policy: A wildlife perspective. *Journal of Environmental Management*, 104, 19–34. <https://doi.org/10.1016/j.jenvman.2012.03.021>
- Ghaderi, A., Shafiekhani, A., & Solaymani, S. (2022). Advanced microstructure and CO gas sensor properties of Cu/Ni bilayers at nanoscale. *Scientific Reports*, 12, Article 16347. <https://doi.org/10.1038/s41598-022-16347-4>



- Gore, A. C., Chappell, V. A., Fenton, S. E., Flaws, J. A., Nadal, A., Prins, G. S., ... & Zoeller, R.T. (2015). EDC-2: The Endocrine Society's second scientific statement on endocrine disrupting chemicals. *Endocrine Reviews*, 36(6), E1–E150. <https://doi.org/10.1210/er.2015-1010>
- Huang, Y. Q., Wong, C. K. C., Zheng, J. S., Bouwman, H., Barra, R., Wahlström, B., & Wong, M. H. (2012). Bisphenol A (BPA) in China: Review of sources, environmental levels, and potential human health impacts. *Environment International*, 42, 91–99. <https://doi.org/10.1016/j.envint.2011.04.010>
- Ibrahim, Q., Creedon, L., & Gharbia, S. (2022). A literature review of modelling and experimental studies of water treatment by adsorption processes on nanomaterials. *Membranes*, 12(4), 360. <https://doi.org/10.3390/membranes12040360>
- International Journal of Environmental Research and Public Health (MDPI). 2020. *Adsorption characteristics and mechanism of Bisphenol A by magnetic biochar. Int. J. Environ. Res. Public Health*, 17(3), 1075. <https://www.mdpi.com/1660-4601/17/3/1075>
- Kang, J. H., Kondo, F., & Katayama, Y. (2006). Human exposure to bisphenol A. *Toxicology*, 226(2–3), 79–89. <https://doi.org/10.1016/j.tox.2006.06.009>
- Katiyar, S., & Katiyar, R. (2023). A comprehensive review on synthesis and application of nanocomposites for adsorption of chromium: Status and future prospective. *Applied Water Science*, 14, Article 11. <https://doi.org/10.1007/s13201-023-02062-6>

- Khan, A. R. (2000). A thermodynamic model for liquid adsorption isotherms. *Separation and Purification Technology*, 20(1–2), 1–10. [https://doi.org/10.1016/s1383-5866\(99\)00065-0](https://doi.org/10.1016/s1383-5866(99)00065-0)
- Kovalskii, A. M., Matveev, A. T., Popov, Z. I., *et al.* (2020). (Ni,Cu)/BN nanohybrids – new efficient catalysts for methanol steam reforming and carbon monoxide oxidation. *Chemical Engineering Journal*, 395, 125109. <https://doi.org/10.1016/j.cej.2020.125109>
- Li, Y., Du, Q., Liu, T., Sun, J., Wang, Y., Wu, S., & Wang, Z. (2019). Removal of bisphenol A using biochar derived from *Cassia siamea* biomass. *Environmental Science and Pollution Research*, 26(3), 2345–2356. <https://doi.org/10.1007/s11356-018-3765-2>
- Liu, J., Zheng, Y., & Hou, S. (2017). Facile synthesis of Cu/Ni alloy nanospheres with tunable size and elemental ratio. *RSC Advances*, 7(60), 38123–38130. <https://doi.org/10.1039/c7ra06062a>
- Mahapatro, A. K. (2022). Energy dispersive X-ray spectroscopy. In *Characterization Techniques for Materials II*. INFLIBNET Centre. <https://ebooks.inflibnet.ac.in/mspl11/chapter/energy-dispersive-x-ray-spectroscopy/>
- Murphy, O. P., Vashishtha, M., Palanisamy, P., & Kumar, K. V. (2023). A review on the adsorption isotherms and design calculations for the optimisation of adsorbent mass and contact time. *ACS Omega*, 8, 17407–17430. <https://doi.org/10.1021/acsomega.2c08155>
- Njud S. Alharbi, Nehad S. Alsubhi, Afnan I. Felimban. (2022) Green synthesis of silver nanoparticles using medicinal plants: Characterization and application.

*Journal of Radiation Research and Applied Sciences*, pg 109-124, ISSN 1687-8507. <https://doi.org/10.1016/j.jrras.2022.06.012>

Orimolade, B. O., Adekola, F. A., Mohammed, A. A., Idris, A. O., Saliu, O. D., & Yusuf, T. (2018). Removal of Bisphenol-A from Aqueous Solution Using Rice Husk Nanosilica: Adsorption Kinetics, Equilibrium and Thermodynamic Studies. *Journal of Applied Chemical Research*, 12(3), 8–21. <https://doi.org/10.22036/jacr.2018.101082.1184>

Ortiz Ortega, E., Hosseinian, H., Rosales López, M. J., Rodríguez Vera, A., & Hosseini, S. (2022). Characterization techniques for chemical and structural analyses. In *Material Characterization Techniques and Applications*. Springer, (pp. 93–152). <https://doi.org/10.1007/978-981-16-9569-84>

Rochester, J. R. (2013). Bisphenol A and human health: A review of the literature. *Reproductive Toxicology*, 42, 132–155. <https://doi.org/10.1016/j.reprotox.2013.08.008>

Rubin, B. S. (2011). Bisphenol A: An endocrine disruptor with widespread exposure and multiple effects. *The Journal of Steroid Biochemistry and Molecular Biology*, 127(1–2), 27–34. <https://doi.org/10.1016/j.jsbmb.2011.05.002>

Santos, R. M. (2022). X-ray diffraction techniques for mineral characterization: A review for engineers of the fundamentals, applications, and research directions. *Minerals*, 12(2), 205. <https://doi.org/10.3390/min12020205>

- Sari, A., Tuzen, M., & Soylak, M. (2009). Adsorption of palladium(II) and platinum(II) from aqueous solution by moss biomass. *Chemical Engineering Journal*, 152(2–3), 389–394. <https://doi.org/10.1016/j.cej.2009.04.013>
- Siddhuraju, P. (2007). Antioxidant activity of polyphenolic compounds extracted from *Cassia siamea* leaves. *Food Chemistry*, 103(1), 31–37. <https://doi.org/10.1016/j.foodchem.2006.07.034>
- Singh, M. J., Nakamura, K., Yoshitake, H., Tewatia, P., Sharma, K., Paulik, C., & Kaushik, A. (2025). Enhanced trace-level assay and excision of Cu (II) ions via MOF-cellulose nanofiber nanohybrids: A study of adsorption mechanism and RSM optimisation. *Journal of Chemical Engineering of Japan*, 58(1), 2527271. <https://doi.org/10.1080/00219592.2025.2527271>
- Singh, R., Gautam, N., Mishra, A., & Gupta, R. (2022). Nanohybrids in environmental remediation: Synthesis, characterization, and applications. *Journal of Environmental Chemical Engineering*, 10(1), 106987. <https://doi.org/10.1016/j.jece.2021.106987>
- Skakri, S., El Attar, A., Benhaiba, S., *et al.* (2025). Facile synthesis of a Ni–Cu composite reinforced with a para-phenylenediamine layer for enhanced hydrogen evolution reaction. *RSC Advances*, 15(30). <https://doi.org/10.1039/d5ra02533h>
- Staples, C. A., Dorn, P. B., Klecka, G. M., O’Block, S. T., & Harris, L. R. (1998). A review of the environmental fate, effects, and exposures of bisphenol A. *Chemosphere*, 36(10), 2149–2174. [https://doi.org/10.1016/S0045-6535\(97\)10133-3](https://doi.org/10.1016/S0045-6535(97)10133-3)

- Tian, H., Gao, Y., & Zhang, Y. (2020). Advanced oxidation processes for BPA degradation: A review. *Chemical Engineering Journal*, 389, 124469. <https://doi.org/10.1016/j.cej.2020.124469>
- Vigdorowitsch, M., Pchelintsev, A., Tsygankova, L., & Tanygina, E. (2021). Freundlich Isotherm: An Adsorption Model Complete Framework. *Applied Sciences*, 11(17), 8078. <https://doi.org/10.3390/app11178078>
- Xue, J., Wan, Y., & Kannan, K. (2021). Occurrence of bisphenol A and its analogues in indoor dust from China and implications for human exposure. *Environmental Science & Technology*, 55(3), 1741–1750. <https://doi.org/10.1021/acs.est.0c06094>
- Yang, Y., Ok, Y. S., Kim, K. H., Kwon, E. E., & Tsang, Y. F. (2017). Occurrences and removal of bisphenol A in wastewater treatment plants: A review. *Environment International*, 106, 135–142. <https://doi.org/10.1016/j.envint.2017.06.010>
- Zhang, W., Zhang, S., Wang, J., & Wang, L. (2021). Adsorption of bisphenol A using metal-organic frameworks: A review. *Journal of Hazardous Materials*, 403, 123676. <https://doi.org/10.1016/j.jhazmat.2020.123676>